DECICE implementation of ship performance in ice: a summary report
Quinton, B.

National Research Council Canada   Conseil national de recherches Canada

Canada

DOCUMENTATION PAGE

REPORT NUMBER SR-2006-06	NRC REPORT NUMBER SR-2006-06	DATE April 2006

REPORT SECURITY CLASSIFICATION Unprotected	DISTRIBUTION Unlimited

TITLE

DECICE IMPLEMENTATION OF SHIP PERFORMANCE IN ICE: A SUMMARY REPORT

AUTHOR(S)

Bruce W. Quinton

CORPORATE AUTHOR(S)/PERFORMING AGENCY(S)

Institute for Ocean Technology, National Research Council, St. John's, NL

PUBLICATION

IOT PROJECT NUMBER PJ2114	NRC FILE NUMBER		

KEY WORDS Discrete element, numerical model, ice, resistance, manoeuvring, turning circle, DECICE	PAGES 60	FIGS. 24	TABLES 10

SUMMARY

DECICE – a discrete element numerical modeling program – has already been proven as a tool for analyzing structure-ice interaction (Lau 1994a, 1994b, 1999 and Lau *et al*., 1996, 2000). The objective of this project is to extend the versatility of DECICE so that it includes modeling of the interactions of vessels with pack ice and level ice. This report summarizes exploration of the feasibility and efficiency of using DECICE to numerically model vessel action in ice environments. The unique characteristics of DECICE and their application to this problem are discussed. The development of standardized numerical model methodology and techniques are presented. Numerical tests for two types of ice performance tests are presented; resistance in pack ice and level ice turning circle tests. Results of these tests are compared with published model tests in order to verify the numerical models.

ADDRESS	National Research Council Institute for Ocean Technology Arctic Avenue, P. O. Box 12093 St. John's, NL A1B 3T5 Tel.: (709) 772-5185, Fax: (709) 772-2462

National Research Council
Canada

Institute for Ocean
Technology

Conseil national de recherches
Canada

Institut des technologies
océaniques

DECICE IMPLEMENTATION OF SHIP PERFORMANCE IN ICE: A SUMMARY REPORT

SR-2006-06

Bruce W. Quinton

April 2006

ACKNOWLEDGMENTS

SUMMARY

DECICE – a discrete element numerical modeling program – has already been proven as a tool for analyzing structure-ice interaction (Lau 1994a, 1994b, 1999 and Lau *et al.*, 1996, 2000). The objective of this project is to extend the versatility of DECICE so that it includes modeling of the interactions of vessels with pack ice and level ice.

This report summarizes exploration of the feasibility and efficiency of using DECICE to numerically model vessel action in ice environments. The unique characteristics of DECICE and their application to this problem are discussed. The development of standardized numerical model methodology and techniques are presented. Numerical tests for two types of ice performance tests are presented; resistance in pack ice and level ice turning circle tests. Results of these tests are compared with published model tests in order to verify the numerical models.

DECICE is the numerical modeling program of choice for these simulations because it employs the "discrete element" numerical method. This method treats elements as distinct entities that interact independently of other elements, and allows elements to fracture, thereby creating new elements. This type of logic allows particle media (i.e. many distinct objects interacting simultaneously – e.g. pack ice) to be modeled very efficiently when compared with the convoluted logic that would be required by a "finite element" numerical modeling program to analyze the same problem.

The numerical models consist of a water foundation, ice elements that are contained by wall elements, and a vessel element. Where possible, measured model test behavioural parameters are used. Where measured parameters are not available, values are either assumed and supported by published literature, or found using sensitivity analyses that measure their effect on the numerical model test results.

Numerical vessel elements are subject to an imposed displacement at constant velocity. This simulates the action of the ice tank test carriage towing the model at constant velocity for each of the model tests.

Two series of published model tests were chosen with which to verify the numerical model: A series of pack ice resistance tests on a conventional lifeboat (TEMPSC) model, and a series of level ice turning circle tests on a model of the CCGS Terry Fox (icebreaker). Matrices of numerical tests identical to their model test counterparts were developed. Results of these tests compare favourably with the published model test results for both ice performance tests types.

TABLE OF CONTENTS

LIST OF FIGURES

LIST OF TABLES

DECICE Implementation of Ship Performance in Ice: A Summary Report

1.0 INTRODUCTION

Numerical models are becoming valuable analysis tools as supplements to model tests. There are several software packages available offering different numerical methods as a basis for simulation of real world phenomena. As part of an ongoing effort to develop numerical modeling techniques, IOT has undertaken the implementation of numerical ice performance tests with DECICE, a discrete element numerical method program.

The objectives and scope of this project are to: 1. Explore the feasibility and efficiency of using DECICE to numerically model vessel-ice interactions in ice environments. 2. Develop standard numerical model methodology and techniques for numerically modeling vessel-ice interactions. 3. Verify the numerical models by conducting simulations of published model tests and comparing the simulation results to the model test results.

DECICE has already been proven as a tool for analyzing structure-ice interaction (Lau 1994a, 1994b, 1999 and Lau *et al.*, 1996, 2000). Extension of the versatility of DECICE to include numerical modeling of the interactions of vessels-in-motion with pack ice and level ice provides an economic supplement to model test predictions. The development of standard methodology and techniques for modeling these types of problems, along with verification of the numerical model provides a basis for routine analysis of problems of this type, and confidence in their results.

Two types of ice performance tests were chosen for numerical modeling: 1. Pack ice resistance tests, and 2. Level ice turning circle tests. The numerical models were verified by comparing simulation test results with published model test data for both of these test series'.

This report consists of four main sections. The first section discusses DECICE, the "discrete element method", and the applicability of both to vessel-ice interaction simulation. The second summarizes the published physical ice performance tests and their results. The third section discusses the development and testing of the numerical model. The final section presents the numerical model verification.

2.0 DECICE AND THE DISCRETE ELEMENT METHOD

DECICE is a commercial numerical modeling program available for three operating systems: VMS®, Sun®, and Windows®. Unlike several popular numerical modeling programs that use the "finite element method", DECICE employs the "discrete element method" as the basis for its simulations.

DECICE was chosen as the engine for these simulations because the discrete element numerical method is an ideal tool for analyzing icebreaking and ice floe interaction. It was created as a tool for analyzing generalized discontinuums like block-jointed rock masses and sea ice floes in which numerous bodies interact and undergo large absolute and relative displacements, rotations, and fracture into new discrete bodies.

The discrete element method treats each element as a distinct body that interacts with other bodies through edge and corner contacts that may change with time.

The governing dynamic equilibrium equations for the discrete elements can be written in the general form:

$$[M]\{\ddot{u}\} + [C]\{\dot{u}\} + [K]\{u\} = \{f\} \tag{1}$$

where: 　　　$\{u\}$ is the displacement matrix (differentiable with time)
　　　　　　$[M]$ is the mass matrix
　　　　　　$[C]$ is the damping matrix
　　　　　　$[K]$ is the stiffness matrix
　　　　　　$\{f\}$ is the applied loads matrix

The relative motion of neighbouring elements dictates the interaction of discrete elements by generating incremental interaction forces given by:

$$\Delta f_n = k_n \Delta u_n + \beta k_n \Delta \dot{u}_n \tag{2a}$$
$$\Delta f_s = k_s \Delta u_s + \beta k_s \Delta \dot{u}_s \tag{2b}$$

where: 　　　β is a stiffness proportional damping coefficient
　　　　　　Δf_n and Δf_s are normal and tangential components of the incremental contact force
　　　　　　k_n and k_s are normal and tangential joint stiffnesses
　　　　　　u_n and u_s are normal and tangential relative joint displacements

One of the major differences between the finite element method and the discrete element method is the number of nodes that comprise the elements. Finite elements "share" common nodes while discrete elements do not. For example, a 2 X 2 two-dimensional lattice of elements under finite element analysis has 9 nodes (see Figure 1): 1 for each external corner (4), 1 for each point where elements meet on the outside edge (4), and 1 for the centre where the mesh lines cross. Only the four external corner nodes are not "shared" with any other elements. The node at the centre of the lattice is

shared by all four finite elements. A similar lattice described with discrete elements has sixteen nodes (see Figure 2): each element has 4 nodes; none of which are shared. The point where the mesh lines cross in the centre of the discrete element lattice is the location of 4 separate nodes. Each node has the same coordinates as the other three (i.e. they occupy the same space). While the four finite elements are "locked" together by virtue of the fact that they share nodes, the discrete elements are not. Under disturbance, they would behave as separate entities, except for the special case in which they are intentionally "locked" together by the user.
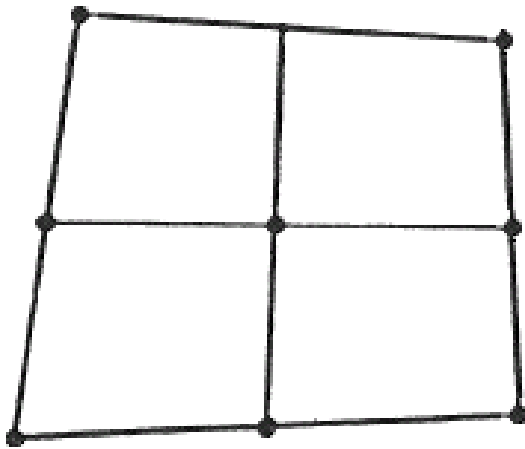
Figure 1: **2 X 2, 2D lattice of finite elements.**
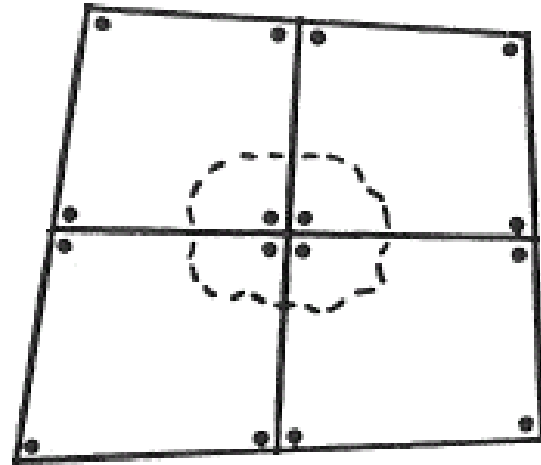
Figure 2: **2 X 2, 2D lattice of discrete elements.**

Discrete element "locking" is used to model an object that is too complex to be described with a single discrete element. The level ice sheets described in this report are examples of such a case. In order to adequately model the icebreaking process that occurs during a turning circle manoeuvre, a level ice sheet was created as a lattice of "locked" discrete elements that had similar geometries as the broken ice pieces observed in the physical model tests. Parameters governing the "breaking away" of the existing "locked" discrete elements and the creation of new discrete elements through element "cracking" are chosen by the user. These features are unique to the discrete element method and provide an efficient method with which to model the icebreaking process.

3.0 ICE PERFORMANCE TESTS

Two types of ice performance tests were simulated: 1. Pack ice resistance tests and 2. Level ice turning circle tests. Both of these performance tests are routinely performed in many ice tanks around the world, for many types of ships, with many different missions. It is the objective of this project that the numerical models developed herein will be useful tools for analyzing and predicting ship performance in ice.

This section outlines two sets of published ice performance model tests and their results. The first set is a series of resistance tests in pack ice (Simões Ré *et al.*, 2003).for a totally enclosed motor propelled survival craft (henceforth referred to as a "conventional lifeboat", or a "TEMPSC"). The second set is a series of level ice turning circle tests for the CCGS Terry Fox (Lau and Derradji-Aouat, 2004).

These sets of published results are compared later in the report with the results of the numerical models in order to verify their validity.

3.1   TEMPSC Resistance Tests in Pack Ice

For a detailed account of these tests and their results, the reader is referred to Simões Ré *et al.* (2003).

3.1.1 Background

Model-scale resistance tests were performed in the Institute for Ocean Technology's ice tank using a 1:13 scale model of a typical 10m long 80-person totally enclosed motor propelled survival craft (TEMPSC) (Figure 3). A summary of the model's hydrostatics is given in Appendix 3 of Simões Ré *et al.* (2003). A tow pole was used to attach the model at its centre of gravity to the ice tank carriage. The model's yaw and sway degrees of freedom were restricted for these tests. Open water and pack ice resistance tests were both performed in the ice tank for ice conditions of varying concentration, size, and thickness.

Figure 3:   Conventional TEMPSC lifeboat 1:13 scale model.

Columnar-grained CD-EG/AD/S ice (Spencer and Timco, 1990) was used for these tests. CD-EG/AD/S stands for "corrected density – ethylene-glycol/aliphatic-detergent/sugar". The density was corrected by bubbling air into the growing ice sheet, thereby improving the scaling properties of the ice. The flexural, compressive, and shear strengths of the model ice were measured frequently throughout the test program. Two 25mm and two 50mm thick (nominal) ice sheets were grown for these tests; corresponding to full-scale nominal ice thicknesses of about 0.325m and 0.650m, respectively. Two sizes of ice floes were modeled: small and large. Ice floe size was controlled by cutting the level ice into strips and breaking them apart by hand. Pack ice concentration was controlled by increasing the water surface area a known amount.

3.1.2 Results

The model test results are shown in Table 1 and a plot of resistance vs. velocity is shown in Figure 4. The names of each test (excluding the open water tests) denote the ice thickness (e.g. H25 is 25mm thick ice) and ice coverage concentration (e.g. C6 is 60% coverage with pack ice). The last column in the table shows the $C_{c,\,pack}$ for the pack ice resistance tests. This is the non-dimensional coefficient of resistance that represents the components of the total resistance that are scalable with Froude scaling (i.e. no viscous component). The frictional (viscous) resistance component, C_f, is subject to scaling according to the ITTC '57 "Ship Model Correlation Line" (ITTC, 1957).
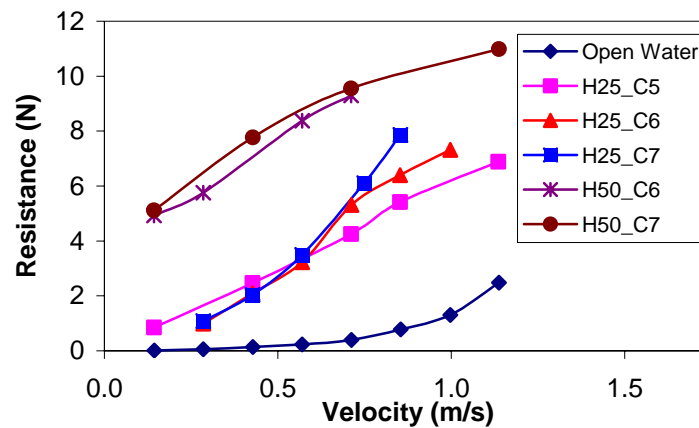
Figure 4:   **Model tests total measured tow force vs. velocity.**

Table 1:   Physical model resistance test results.

Legend	V [m/s]	R_T [N]	Re	C_F	R_F [N]	$R_{c,pack}$ [N]	Fn_i	$C_{c,pack}$
Open Water	0.144	0.845	8.565E+04	0.00872	---	---	---	---
2	0.285	0.883	1.695E+05	0.00719	---	---	---	---
3	0.428	0.974	2.546E+05	0.00647	---	---	---	---
4	0.570	1.059	3.390E+05	0.00602	---	---	---	---
5	0.712	1.228	4.235E+05	0.00570	---	---	---	---
6	0.854	1.615	5.079E+05	0.00546	---	---	---	---
7	0.997	2.131	5.930E+05	0.00527	---	---	---	---
8	1.137	3.309	6.763E+05	0.00511	---	---	---	---
M13_H25_C5	0.143	0.854	8.486E+04	0.00874	0.017	0.836	0.378	90.744
2	0.427	2.473	2.538E+05	0.00647	0.115	2.358	1.130	28.616
3	0.711	4.256	4.231E+05	0.00570	0.281	3.975	1.884	17.356
4	0.852	5.412	5.069E+05	0.00546	0.387	5.025	2.258	15.281
5	1.136	6.884	6.756E+05	0.00511	0.643	6.241	3.009	10.685
M13_H25_C6	0.285	0.986	1.696E+05	0.00719	0.057	0.929	0.690	14.595
2	0.427	2.092	2.540E+05	0.00647	0.115	1.977	1.033	13.864
3	0.570	3.230	3.390E+05	0.00602	0.191	3.040	1.378	11.962
4	0.712	5.312	4.233E+05	0.00570	0.281	5.030	1.721	12.698
5	0.852	6.401	5.070E+05	0.00546	0.387	6.014	2.061	10.580
6	0.997	7.318	5.931E+05	0.00527	0.511	6.808	2.412	8.752
M13_H25_C7	0.285	1.089	1.697E+05	0.00719	0.057	1.032	0.639	10.211
2	0.427	2.042	2.540E+05	0.00647	0.115	1.927	0.956	8.510
3	0.570	3.497	3.393E+05	0.00602	0.191	3.306	1.277	8.182
4	0.749	6.105	4.453E+05	0.00563	0.308	5.797	1.676	8.327
5	0.853	7.860	5.076E+05	0.00546	0.388	7.473	1.911	8.261
M13_H50_C6	0.143	4.931	8.529E+04	0.00873	0.017	4.914	0.269	186.603
2	0.285	5.761	1.693E+05	0.00719	0.057	5.704	0.534	54.945
3	0.570	8.371	3.388E+05	0.00602	0.190	8.181	1.068	19.691
4	0.711	9.296	4.231E+05	0.00570	0.281	9.015	1.334	13.912
M13_H50_C7	0.143	5.120	8.497E+04	0.00874	0.017	5.103	0.248	122.941
2	0.428	7.773	2.544E+05	0.00647	0.115	7.658	0.743	20.582
3	0.711	9.549	4.231E+05	0.00570	0.281	9.268	1.236	9.004
4	1.137	10.981	6.761E+05	0.00511	0.644	10.337	1.974	3.933

The discrepancy between this table and Table 8.3, P. 23 as reported in Simões Ré *et al*. (2003) is due to the fact the ice density was used to calculate frictional resistance (R_F) instead of water density. This oversight is corrected in Table 1.

3.1.3 Scaling and data manipulation

The scaling procedures are outlined in detail in Lau and Simões Ré. (2006). The predicted full-scale model test results are presented here in Table 2.

The numerical simulations were carried out without simulating hydrodynamic drag on the vessel element. Accordingly, the open water model test results were used to remove the hydrodynamic effects from the total model test resistances.

To do this, a 5th order regression of the open water test results was performed which yielded the velocity dependent hydrodynamic resistance equation:

$$R_{ow} = 21.5V^5 - 154V^4 + 440V^3 - 418V^2 + 217V \qquad [kN] \tag{3}$$

A plot of the hydrodynamic resistance regression is shown below in Figure 5.

$$R_{OW} = 21.484V^5 - 154.44V^4 + 439.92V^3 - 418.01V^2 + 217.42V$$
$$R^2 = 0.999$$
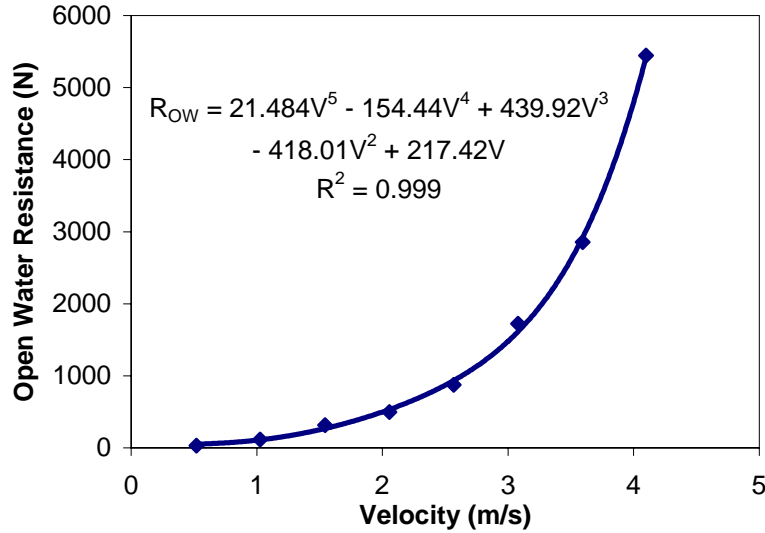
Figure 5: **Full scale open water resistance regression.**

The hydrodynamic resistance was then removed from the total resistance for each pack ice resistance test using the following equation.

$$R_c = R_T - R_{OW} \tag{4}$$

R_C was the resistance value used to verify the results of the numerical pack ice resistance model, and its predicted values for each run are shown in the last column of Table 2.

Table 2:   **Predicted full-scale model pack ice resistance test results.**

| Test Name | Full Scale | | |
	Velocity [m/s]	Total Resistance [N]	Ice Component Resistance [N]
Open Water	0.519	32	---
2	1.028	116	---
3	1.543	316	---
4	2.055	496	---
5	2.567	874	---
6	3.079	1724	---
7	3.595	2858	---
8	4.100	5446	---
M13_H25_C5	0.516	1876	1825
2	1.540	5433	5163
3	2.564	9350	8399
4	3.072	11890	10245
5	4.096	15124	9572
M13_H25_C6	1.028	2166	2054
2	1.540	4596	4326
3	2.055	7096	6556
4	2.567	11670	10715
5	3.072	14063	12418
6	3.595	16078	13070
M13_H25_C7	1.028	2393	2281
2	1.540	4486	4217
3	2.055	7683	7142
4	2.701	13413	12312
5	3.076	17268	15617
M13_H50_C6	0.516	10833	10782
2	1.028	12657	12545
3	2.055	18391	17850
4	2.564	20423	19472
M13_H50_C7	0.516	11249	11198
2	1.543	17077	16806
3	2.564	20979	20028
4	4.100	24125	18548

3.2 Level Ice Turning Circle Tests

A detailed treatment of these tests and their results can be found in Lau and Derradji-Aouat (2006).

3.2.1 Background

Model-scale level ice turning circle tests were performed at IOT's ice tank using a 1:21.8 scale model of the CCGS Terry Fox, shown in Figure 6. The model's hydrostatics are given in the Appendix A in Lau and Derradji-Aouat (2006). The model was attached to the ice tank carriage using the PMM (Marineering Ltd., 1997). The PMM was attached at the model's centre of gravity and the roll degree of freedom was restricted. Open

water and level ice turning circle tests were both performed in the ice tank for turning circle radii of 10 [m], 50 [m], and infinite (straight line).

Figure 6:   CCGS Terry Fox model attached to the PMM.

Columnar-grained CD-EG/AD/S ice was also used for these tests. The flexural, compressive, and shear strengths of the model ice were measured frequently throughout the test program. All level ice tests were conducted in ice of nominal flexural strength and thickness of 35 [kPa] and 40 [mm] respectfully.

3.2.2 Results

The numerical simulations of these level-ice turning circle tests were carried out at model-scale; therefore scaling of these tests results was not necessary.

The results of the Terry Fox level ice turning circle tests, presented in Lau and Derradji-Aouat (2006), are summarized here in Table 3. Note: the "straight line" open water and level ice "Mean Tow Force" values are taken from another identical test series (Derradji-Aouat and van Thiel, 2004).

Table 3:   Terry Fox turning circle ice performance model test results.

Test	R [m]	Model Velocity [m/s]	Mean Tow Force [N]	Yaw Moment [Nm]
Open Water	inf	0.1	0.32	---
Open Water	inf	0.3	2.08	---
Open Water	inf	0.6	7.43	---
Open Water	inf	0.9	16.05	---
Open Water	10	0.1	---	0.93
Open Water	10	0.3	---	-0.63
Open Water	10	0.6	---	-7.96
Open Water	10	0.9	---	-21.02
Open Water	50	0.1	---	0.07
Open Water	50	0.3	---	-0.9
Open Water	50	0.6	---	-4.47
Open Water	50	0.9	---	-10.41
Level Ice	inf	0.02	20.47	---
Level Ice	inf	0.1	27.77	---
Level Ice	inf	0.3	40.77	---
Level Ice	inf	0.6	52.07	---
Level Ice	10	0.05	---	67.91
Level Ice	10	0.1	---	77.58
Level Ice	10	0.2	---	84.26
Level Ice	10	0.3	---	113.52
Level Ice	10	0.4	---	93.42
Level Ice	10	0.5	---	114.19
Level Ice	10	0.6	---	123
Level Ice	50	0.02	---	15.86
Level Ice	50	0.1	---	38.24
Level Ice	50	0.3	---	25.96
Level Ice	50	0.6	---	84.81

4.0 DEVELOPMENT AND TESTS OF THE NUMERICAL MODELS

Like physical model tests, limits exist on the potential and feasibility of any numerical simulation. There is a direct relationship between the number of elements in a simulation, and the amount of computing power and computing time required to perform that simulation. For example, modeling an infinite ice sheet would require infinite ice elements, infinite computing power, and infinite computing time. Also, because explicit-explicit time stepping (Intera Information Technologies, 1986) is required for these types of simulations, a very small time step is required to maintain simulation stability. Stiffness parameters (e.g. element interaction stiffness) have a direct impact on the efficiency of a numerical simulation. High stiffness values tend to decrease the time step length, thereby requiring more time steps and computational time to analyze the same simulation time.

In designing the following numerical test procedures, it was necessary to impose the same constraints, behavioural parameters, and disturbance parameters as were present in the physical model tests. Since the both ice performance test types were performed an ice tank, they share many common features.

The unique features for each numerical test set-up will be discussed in the next section, followed by their common features.

4.1   Pack Ice Resistance Test Numerical Model

The unique features of the pack ice resistance tests' numerical simulations are outlined below.

4.1.1 Coordinate system

The global coordinate system used in these simulations is located with the x-origin at the aft most point of the initial position of the ship element (at t = 0 s) with its positive direction pointing in the direction of the ship's initial motion, the z-origin is at waterline elevation with its positive direction pointing vertically upward, and the y-origin is located at the intersection of the x and z axes with its direction governed by the right-hand rule (RHR).

The origin of the local coordinate system for the lifeboat model is located at the element's centre of gravity (CG) with the positive x-axis pointing toward the bow along the centreline of the vessel, the positive z-axis pointing vertically upward, and the positive y-axis pointing to port (RHR). This local coordinate system translates and rotates with the ship element.

4.1.2 Required numerical elements

The elements required for this numerical model are: 1. The lifeboat element, 2. The pack ice elements, 3. The rigid wall boundary elements, and 4. The water foundation. These four major parts of the numerical model are shown in Figure 7.
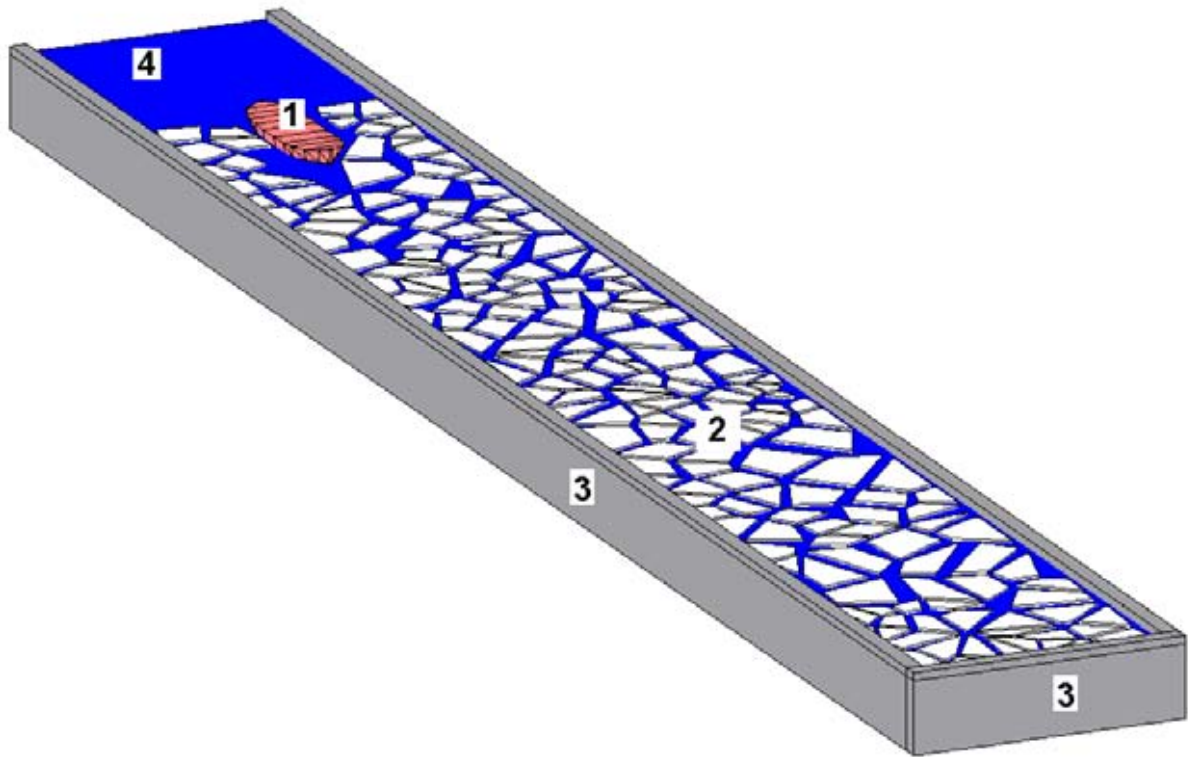
Figure 7: **Required pack ice resistance test numerical model elements.**

For a detailed treatment of the design and development of these numerical elements, the reader is referred to Lau and Henley (2004) and Quinton (2004).

TEMPSC element
The conventional lifeboat was numerically modeled as a *motion element* (ME). A motion element is a rigid element that is capable motion in six degrees of freedom. It was modeled as a rigid element because structural analysis of the model's hull was not a requirement for these tests. The lifeboat element's geometry consists of a collection of adjacent three and four sided polygons. This geometry can be seen in Figure 8.
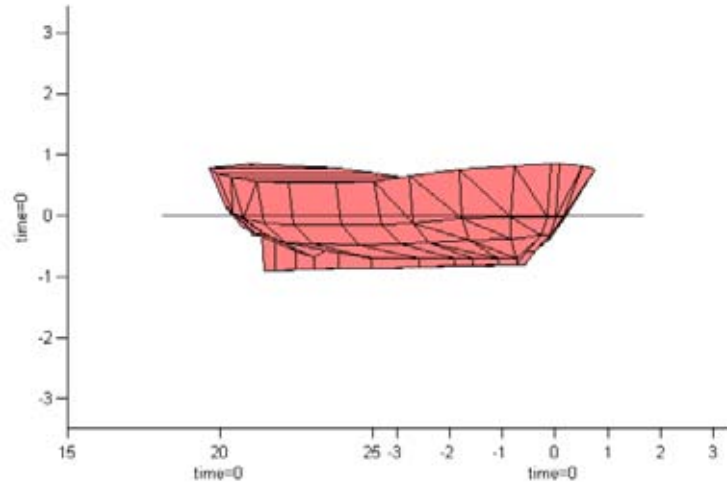
Figure 8:   **Numerical representation of conventional lifeboat hull.**

The hydrostatics and mass properties of the lifeboat model used in the physical tests are given in Table 4. These values were used to construct the lifeboat element (Lau and Henley, 2004). Hydrodynamic characteristics matching of the lifeboat element with the physical model was necessary due to the inherent error associated with representing curved surfaces numerically (i.e. with a collection of three and four sided polygons). This was accomplished through a series of numerical ballast, trim, decay, and open water tests. The longitudinal centre of gravity and vessel's mass were iterated until the draft, trim, and natural frequency characteristics satisfactorily matched the physical model's values (Lau and Henley (2004)).

Table 4:   **Hydrostatic and mass properties of conventional lifeboat.**

		Full Scale	1:13 Scale
Length Overall	(m)	10.0	0.769
Beam at Mid-Ship	(m)	3.30	0.259
Displacement	(kg)	11800	5.38
Longitudinal Centre of Gravity	(m)	4.98	0.383
Vertical Centre of Gravity	(m)	1.34	0.103
Draft at Mid-Ship	(m)	0.897	0.069

Ice elements
Ice floes were simulated using *simply deformable finite elements* (SDFE's). These elements can normally be deformed, bent, and/or broken during interaction with their surroundings, but because icebreaking was not a consideration during these tests, only element deformation was allowed. Pack ice floe sheets of specified concentrations, floe areas, and thicknesses were randomly generated using Tess2D, an in-house tessellation program (Schachter, 1993). Figure 9 shows a typical pack ice sheet with some ice elements removed to allow the vessel element to start its run within the pack ice.

13
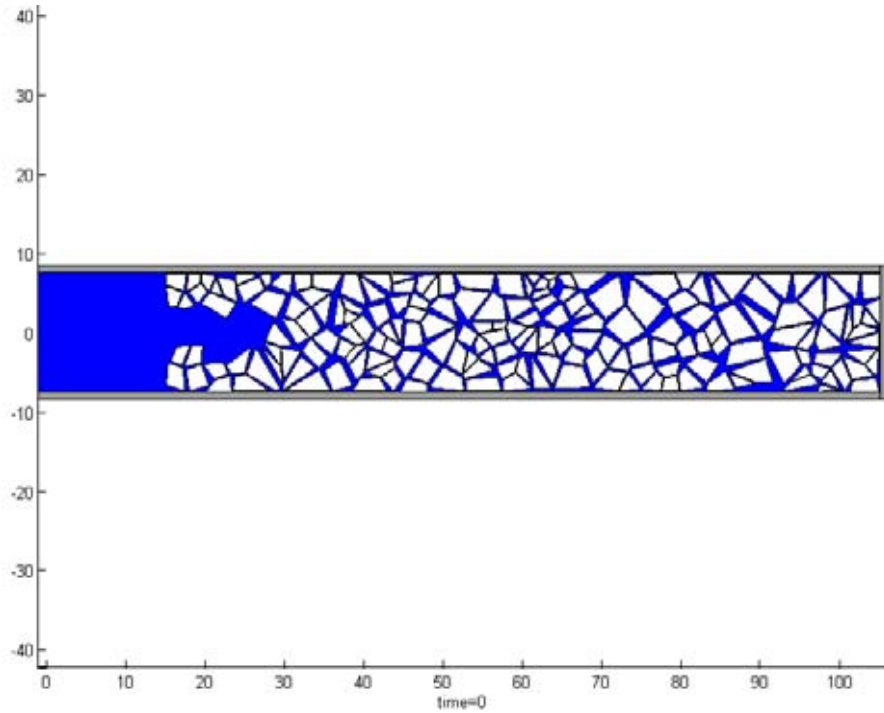
Figure 9: **Pack ice elements.**

Tess2D reduces a rectangle of known size into a group of convex polygons of random size such that the sum of the areas of the polygons divided by the initial rectangular area gives the desired concentration of pack ice.

Due to the way Tess2D generates the random floe geometries, an iterative process was required to obtain pack ice sheets that were within the target parameters and acceptable error limits.

Wall boundaries

The wall boundaries were modeled with rigid elements that were fixed in all degrees of freedom. They extended above and below the water surface in order to contain the ice floes in the same manner as ice tank walls restrict them during model tests.

Water foundation
In all cases the water density used was the ice tank water density, 1002.4 kg/m³.

Numerical modeling of the effects of water on the behaviour of the ice elements was accomplished using the drag coefficient (C_D). The drag coefficient is applied using the PHYSICAL-CONST card. It applies a universal velocity dependant drag to all elements that are not subject to imposed velocities. Water drag is modeled using the equation:

$$F_D = \frac{C_D V_e^2 \rho_w A_v}{2}$$

(5)

14

$$P_D = \frac{C_D \omega^2 \rho_w A_\omega}{2}$$

$\qquad\qquad\qquad\qquad\qquad\qquad\qquad\qquad\qquad\qquad\qquad\qquad$ (6)

where:$\qquad$$C_D$ = the drag coefficient

$\qquad\qquad\qquad\qquad$$V_e$ = the velocity of the element

$\qquad\qquad\qquad\qquad$$\omega$ = the angular velocity of the element

$\qquad\qquad\qquad\qquad$$\rho_w$ = the density of water

$\qquad\qquad\qquad\qquad$$A_v$ and A_ω = element projected "areas" for the vessel element

Use of the drag coefficient may cause instability in some simulations, eventually causing them to crash before completion. Output obtained before the crash is still usable, however the simulation time may be shorter than desired. This instability issue is currently being investigated. Use of C_D is the preferred method of applying water drag to ice elements.

Hydrodynamic drag can be applied to the lifeboat element using the HYDRO-DAMP card. With this card it is possible to simulate the hydrodynamic effects of water on a *motion element* (i.e. the lifeboat element) using a 5th degree polynomial (where resistance is dependent on element velocity) and added mass coefficients. Results of the physical open water resistance tests and decay tests for the physical lifeboat model were used by Lau and Henley (2004) to determine the resistance vs. velocity and added mass characteristics of the lifeboat element. Unfortunately, applying a constant velocity to an element negated the effects of the velocity dependent HYDRO-DAMP card. Therefore it was not possible to model the hydrodynamic effects of water on the lifeboat element. The numerical simulations were carried out considering only the ice component of resistance. Note that the HYDRO-DAMP card can be used on a motion element in conjunction with an applied force.

4.2   Level Ice Turning Circle Test Numerical Model

The unique features of the level ice turning circle tests' numerical simulations are outlined below.

4.2.1   Coordinate system

The global coordinate system used in these numerical simulations initially has its origin along the ship element's centreline, at the waterline, above the longitudinal centre of gravity. The positive global x-direction points in the direction of the vessel's initial motion, the positive global z-direction points vertically upward, and the positive global y-direction points to port (as governed by the right-hand rule (RHR)).

The origin of the local coordinate system for the ship element is located at the element's centre of gravity (CG) with the positive x-axis pointing toward the bow along the centreline of the vessel, the positive z-axis pointing vertically upward, and the positive y-axis pointing to port (RHR). This local coordinate system translates and rotates with the element.

4.2.2 Required numerical elements

The elements required for this numerical model are: 1. The model scale Terry Fox element, 2. The level ice sheet element(s), 3. The wall boundary elements, and 4. The water foundation. These four major parts of the numerical model are shown in Figure 10.
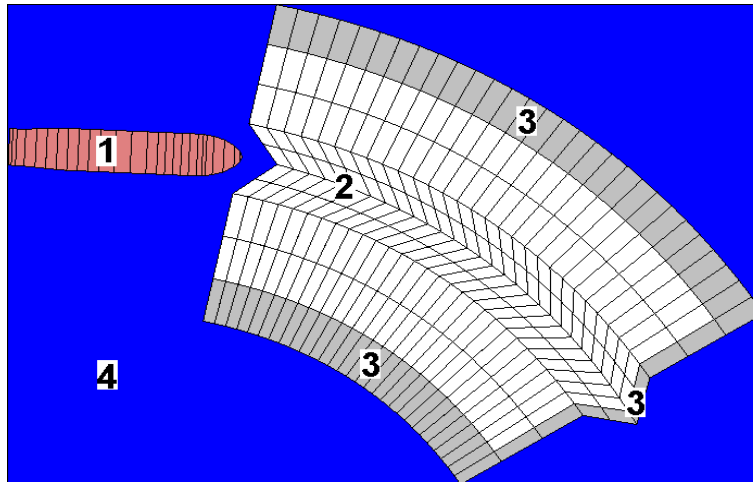
Figure 10:   **Required level ice turning circle numerical model elements.**

Terry Fox element
The CCGS Terry Fox, a Canadian Coast Guard icebreaker, was numerically modeled in model-scale (λ = 21.8) as a *motion element* (Lau and Henley, 2004). The Terry Fox element's geometry is shown in Figure 11.
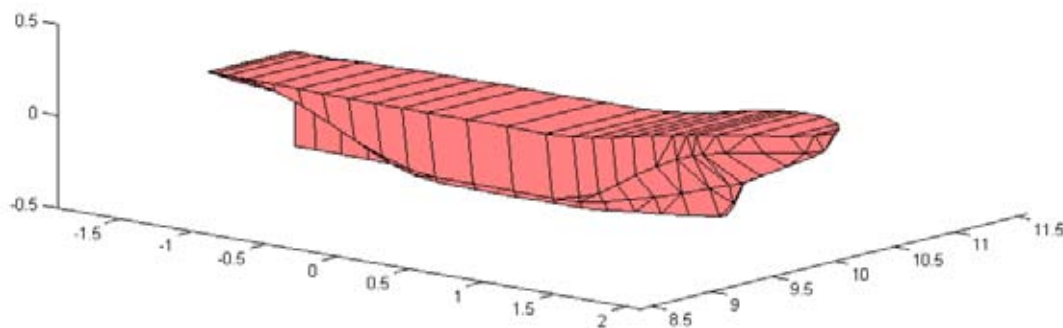
Figure 11:   **Numerical representation of Terry Fox model.**

Similar to the generation of the TEMPSC element (described in Section 4.1.2), the hydrostatics (shown in Table 5) were used to create the element geometry and the results of model ballast, trim, and open water tests were used to match its hydrodynamics to those of the physical model. Numerical decay tests were not considered in these simulations because only forward motion was modeled.

16

Table 5: **Hydrostatic and mass properties of the Terry Fox model.**

		Full Scale	1:21.8 Scale
Length Overall	(m)	88.00	4.037
Beam at Mid-Ship	(m)	17.48	0.802
Displacement	(kg)	7.07E+06	682.3
Longitudinal Centre of Gravity	(m)	31.22	1.432
Vertical Centre of Gravity	(m)	6.730	0.3087
Draft at Mid-Ship	(m)	8.200	0.3762

Ice elements

Ice floes were simulated using *simply deformable finite elements*. Icebreaking was being modeled in these simulations, therefore element deformation, bending, and breaking along locked element faces (i.e. mesh lines) were allowed.

Level ice sheets consisting of two ice material types were created for each test run. The first ice material type was used to construct the mesh of elements that were not subject to direct interaction with the Terry Fox element. These elements are referred to as the "outside ice" elements. The second ice material type was used to construct the mesh of elements that were subject to direct contact with the Terry Fox element. These elements are referred to as the "channel ice" elements. Material properties for both ice types were identical except for the mass damping applied to each: 10% critical mass damping was applied to the "channel ice" elements and 5% critical mass damping was applied to the "outside ice" elements.

A typical level ice sheet is shown in Figure 12. The "channel ice" is distinguished by its chevron shape, and the "outside ice" is present on either side.
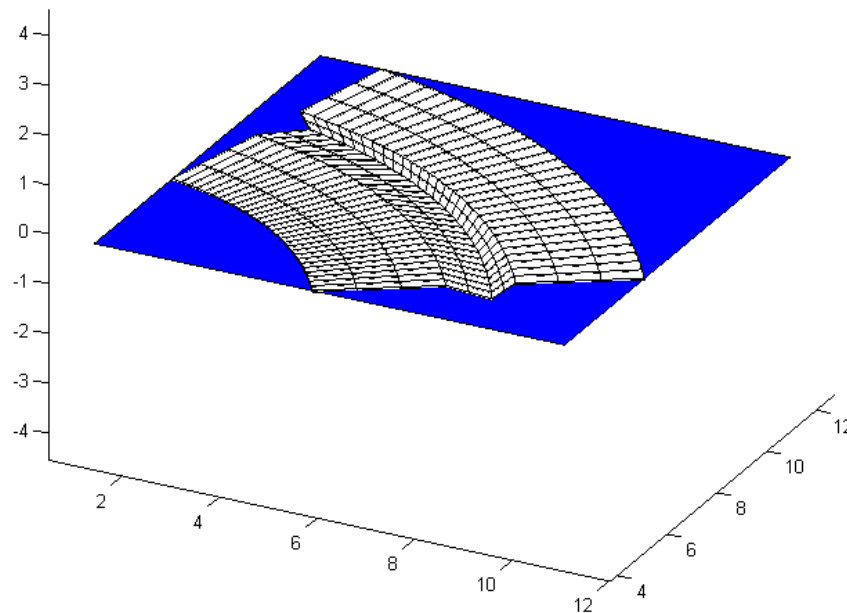
Figure 12: **Typical numerical level ice sheet.**

Wall boundaries
Since level ice is not composed of a collection of discontinuous media, rigid wall boundaries in the sense that they were used for the pack ice resistance tests were not necessary. For these simulations, fixing the outermost ice elements in all degrees of freedom was sufficient to contain the level ice sheet. The fixed boundaries are shown in grey in Figure 13.
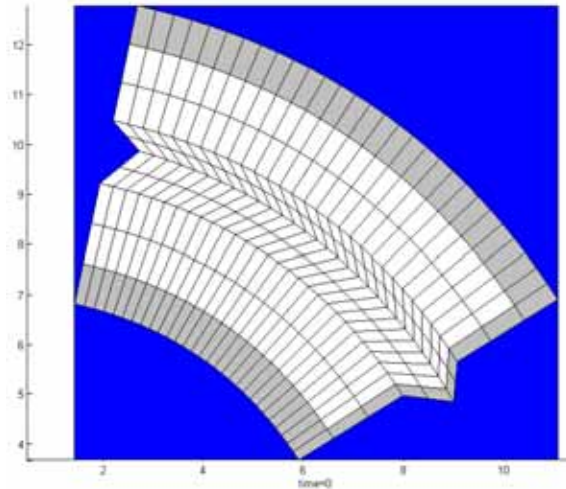
Figure 13:   Level ice sheet wall boundaries.

Water simulation
For all numerical simulations, the water density used was the ice tank water density, 1002.4 kg/m^3. Numerical modeling of the effects of water drag on the behaviour of the ice elements was accomplished using mass damping. Again, the hydrodynamic resistance on the Terry Fox element was not modeled.

The DAMPING-MAT card was used to apply water drag effects to the "outside ice" and "channel ice" elements as discussed above. Mass damping can simulate water effects by causing elements to damp the energy transferred to them as if they were in water. Because the elements of each material type are relatively equal in size, it was possible to apply mass damping without the possibility of over-damping or under-damping an elements motion.

4.3   Commonalities of the Numerical Models

All physical model tests were carried out in a similar environment, giving rise to similarities in between numerical simulation of each type of ice performance test.

Slight geometric differences exist between the physical model and the numerical model vessels. The nature of numerical modeling requires that curved surfaces (such as those on the physical model vessels) be approximated with three and four sided polygons. There are no restrictions on the number of polygons that can be used to

define an element and great effort went into ensuring that the numerical vessel models were sufficiently accurate.

Most behavioural and disturbance parameters were common between all simulations as well. These are outlined in the following two subsections.

4.4 Behavioural Parameters

Behavioural parameters (Moaveni, 1999) are material and environmental properties that influence the behaviour of the numerical elements. Material properties include density, Young's Modulus, Poisson's Ratio, natural frequency, internal friction angle, compressive strength, flexural strength, and tensile strength. Environmental properties include the gravitational constant, element interaction stiffness, element interaction friction, and element interaction cohesion.

The implementation of these behavioural parameters into the numerical model can be broken into three categories: measured values, assumed values, and determined values.

4.4.1 Measured values

Where possible, values measured during the physical model tests were incorporated into the numerical model. These known values served as a basis for determining the other behavioural parameters that were not possible to measure.

The known behavioural parameters were:

Known Parameter	Value
Water Density [kg/m^3]	1002.4
Gravitational Constant [m/s^2]	-9.81
Ice Density [kg/m^3] (variable)	850.0, 868.0, 881.0
Ship/Hull Friction Coeff. (variable)	0.4, 0.2
Ice Young's Modulus [Pa] (variable)	1.11E+08, 1.0E+09
Compressive Strength [Pa]	0.13E+06
Flexural Strength [Pa]	0.315E+05

4.4.2 Assumed values

Where it was not possible to use measured values, some values could be assumed and supported by published literature. These include:

Assumed Parameter	Value
Ice Poisson's Ratio [non-dim]	0.3
Ice Internal Friction Angle [DEG]	30.0
Ice Tensile Strength [Pa]	0.315E+05
Minimum Element Volume [m^3]	0.00525
Ice % Critical Mass Damping	5%, 10%
Ice % Critical Internal Damping	70%

4.4.3 Determined values

Some parameters were peculiar to DECICE and were subject to sensitivity studies to determine their impact on the simulation results. These values include *viscous drag*, *element interaction stiffness* (known to DECICE as INTER-STIFF), and rigid wall boundary/pack ice *separation distance* (pack ice resistance numerical model only). These parameters are explored in the next section.

4.4.4 Sensitivity Analysis

Element interaction stiffness (INTER-STIFF)
The element interaction stiffness parameter directly influences the transfer of energy between discrete elements. Of interest in these numerical models is its effect on the energy transfer when the ship element impacts the ice element.

A series of tests was carried out to examine the sensitivity of the pack ice numerical model to variance in the element interaction stiffness. The test matrix is shown in Table 6.

Table 6:   **Element interaction stiffness sensitivity test matrix for pack ice resistance numerical model.**

Filename	velocity.x	INTER-STIFF
vk_var_16	0.520	1.0E+05
vk_var_17	0.520	1.0E+06
vk_var_18	0.520	1.0E+07
vk_var_19	0.520	1.0E+08
vk_var_20	0.520	1.0E+09
vk_var_01	1.540	1.0E+05
vk_var_02	1.540	1.0E+06
vk_var_03	1.540	1.0E+07
vk_var_04	1.540	1.0E+08
vk_var_05	1.540	1.0E+09
vk_var_06	2.564	1.0E+05
vk_var_07	2.564	1.0E+06
vk_var_08	2.564	1.0E+07
vk_var_09	2.564	1.0E+08
vk_var_10	2.564	1.0E+09
vk_var_21	3.600	1.0E+05
vk_var_22	3.600	1.0E+06
vk_var_23	3.600	1.0E+07
vk_var_24	3.600	1.0E+08
vk_var_25	3.600	1.0E+09
vk_var_11	4.096	1.0E+05
vk_var_12	4.096	1.0E+06
vk_var_13	4.096	1.0E+07
vk_var_14	4.096	1.0E+08
vk_var_15	4.096	1.0E+09

These tests were carried out in 0.50 [m] thick pack ice, at 6/10ths concentration, and at various velocities. The results shown in Figure 14 correspond to a run distance of 3 lifeboat lengths with spring stiffnesses ranging from 1x106 N/m^2 to 1x108 N/m^2. For these runs, the drag coefficient was set to zero. Because the choice of element interaction stiffness affects the computational efficiency and stability of the numerical model, not all of the tests yielded useable results. Figure 14 shows that within the range tested, element interaction stiffness does not significantly affect the outcome of the ship element resistance. This gives freedom to select a lower spring constant within the examined range of stiffness for computation efficiency.
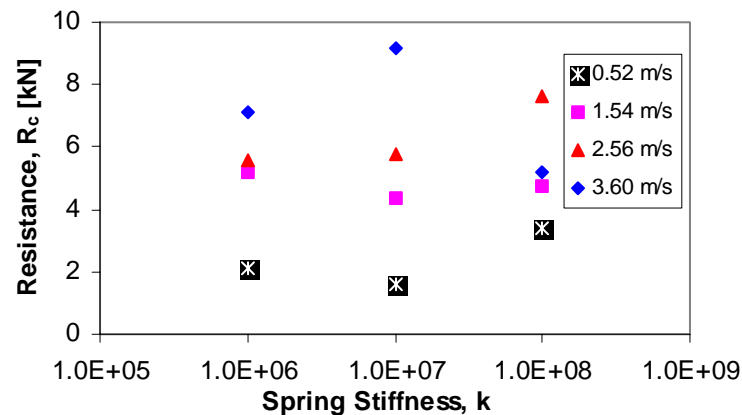
Figure 14:   **The influence of element interaction stiffness on pack ice resistance.**

Normal and tangential INTER-STIFF values of 1x10^7 N/m^2 (for each) were chosen for the pack ice resistance numerical model, These values are consistent with those used in Babic´ *et al.* (1990), Savage (1992), and Løset (1994). Based on experience with the above tests, values of 3x10^6 and 2.8x10^5 (for normal and tangential INTER-STIFF values respectfully) were chosen for the level ice turning circle numerical model.

Drag Coefficient
The drag coefficient parameter directly influences the amount of work done on ice elements as they move through a fluid with velocity. Of interest in these numerical models is its effect on the resistance transferred to the ship element during impacts with ice elements.

A series of tests was carried out to examine the sensitivity of the pack ice numerical model to variance in the element interaction stiffness. The test matrix is shown in Table 7.

Table 7:   **Drag coefficient sensitivity test matrix for pack ice resistance numerical model.**

Filename	Velocity	CD
Drag_VAR_01	1.540	0.00
Drag_VAR_02	1.540	0.25
Drag_VAR_03	1.540	0.50
Drag_VAR_04	1.540	0.75
Drag_VAR_05	1.540	1.00
Drag_VAR_06	1.540	1.25
Drag_VAR_07	1.540	1.50
Drag_VAR_08	2.564	0.00
Drag_VAR_09	2.564	0.25
Drag_VAR_10	2.564	0.50
Drag_VAR_11	2.564	0.75
Drag_VAR_12	2.564	1.00
Drag_VAR_13	2.564	1.25
Drag_VAR_14	2.564	1.50
Drag_VAR_15	4.096	0.00
Drag_VAR_16	4.096	0.25
Drag_VAR_17	4.096	0.50
Drag_VAR_18	4.096	0.75
Drag_VAR_19	4.096	1.00
Drag_VAR_20	4.096	1.25
Drag_VAR_21	4.096	1.50
Drag_VAR_22	0.540	0.00
Drag_VAR_23	0.540	0.25
Drag_VAR_24	0.540	0.50
Drag_VAR_25	0.540	0.75
Drag_VAR_26	0.540	1.00
Drag_VAR_27	0.540	1.25
Drag_VAR_28	0.540	1.50
Drag_VAR_29	3.600	0.00
Drag_VAR_30	3.600	0.25
Drag_VAR_31	3.600	0.50
Drag_VAR_32	3.600	0.75
Drag_VAR_33	3.600	1.00
Drag_VAR_34	3.600	1.25
Drag_VAR_35	3.600	1.50

The effect of the various drag coefficients on ship element resistance is demonstrated in Figure 15. These sensitivity tests were performed using the pack ice resistance numerical model with 37.83 cm thick pack ice of 2.21 [m] average diameter, 5/10ths pack ice concentration, and at various ship speeds. An INTER-STIFF value of $1x10^7$ [N/m] and a run distance of 3 ship lengths were used in these tests. As shown in the figure, the drag coefficient has negligible influence on lifeboat resistance for these runs Lau and Simões Ré, 2006). This trend is expected because the transfer of drag force to the lifeboat element would be limited to the initial impact.
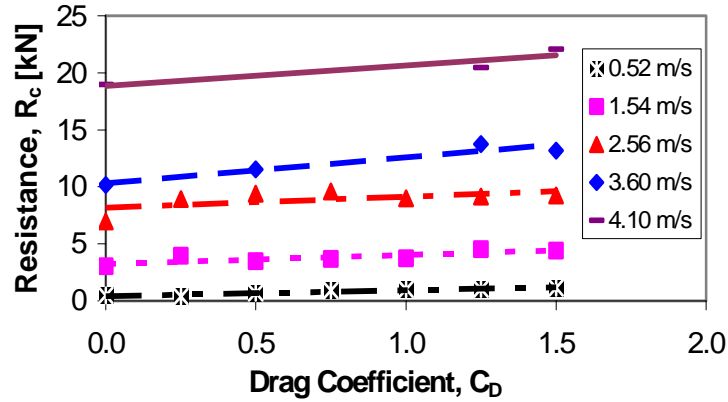
Figure 15: The influence of drag coefficient on pack ice.

A value of 1.3 was selected for the drag coefficient for the pack ice resistance test simulations.

4.5 Disturbance Parameters

Disturbance parameters (Moaveni, 1999) take the form of either applied loadings or applied displacements (and their derivatives). The nature of the physical model tests being simulated is such that an applied constant velocity is the necessary choice. This is because the both model test series' were conducted at a constant velocity through a combination of the motions of the ice tank carriage and the planar motion mechanism. The models were never propelled under their own power (in which case an applied loading would be the best disturbance alternative).

Constant velocities were applied in these simulations using the VELOC-DEFN and RVELO-DEFN cards. The VELOC-DEFN card is used to define the initial velocity state of the ship element, at time t = 0 [s]. The RVELO-DEFN card is used to define the velocity during the simulation (i.e. for time t > 0 [s]).

5.0 NUMERICAL MODEL VERIFICATION

In order to verify the numerical models, simulations of published model tests were performed and their results compared with the results of their respective model tests. A summary of the verification process and results is presented in this section.

As a supplement to this report, and particularly this section, the papers published for POAC '06 (Lau and Simões Ré, 2006 - pack ice resistance simulations) and IAHR '06 (Lau, 2006 - level ice turning circle simulations) are included in this report as Appendix A and Appendix B respectfully.

5.1   Numerical Model Tests

Simulations for both ice performance tests types were set-up according to the ideology, techniques, and parameters defined in Section 4. Simulation test matrices were identical to their physical model counterparts.

5.1.1   Test matrices

Table 8 and Table 9 show the test matrices for both numerical model verification test series'. These matrices correspond directly with their physical model counterparts.

Table 8:   **Pack ice resistance test matrix**

Test Number	V_s [m/s]	Full Scale Ice Thickness [mm]	Full Scale Conc. [1/10th]
M13_H25_C5	0.516	325	5
2	1.54	325	5
3	2.564	325	5
4	3.072	325	5
5	4.096	325	5
M13_H25_C6	1.028	325	6
2	1.54	325	6
3	2.055	325	6
4	2.567	325	6
5	3.072	325	6
6	3.595	325	6
M13_H25_C7	1.028	325	7
2	1.54	325	7
3	2.055	325	7
4	2.701	325	7
5	3.076	325	7
M13_H50_C6	0.516	650	6
2	1.028	650	6
3	2.055	650	6
4	2.564	650	6
M13_H50_C7	0.516	650	7
2	1.543	650	7
3	2.564	650	7
4	4.1	650	7

Table 9:   Level ice turning circle test matrix

Run	R [m]	Drift Angle [DEG]	V [m/s]
SM99_0_02	INF	0	0.02
SM99_0_10	INF	0	0.1
SM99_0_30	INF	0	0.3
SM99_0_60	INF	0	0.6
SM10_0_02	10	0	0.02
SM10_0_10	10	0	0.1
SM10_0_30	10	0	0.3
SM10_0_60	10	0	0.6
SM50_0_02	50	0	0.02
SM50_0_10	50	0	0.1
SM50_0_30	50	0	0.3
SM50_0_60	50	0	0.6
SM10_0_05	10	0	0.05
SM10_61_30	10	0.61	0.2
SM10_114_60	10	1.14	0.3
SM10_174_02	10	1.74	0.42
SM10_270_10	10	2.7	0.5
SM10_380_30	10	3.8	0.6
SM50_07_10	50	0.07	0.1
SM50_19_30	50	0.19	0.3
SM50_54_60	50	0.54	0.6

All tests shown were performed and compared with their respective physical model test.

5.1.2 Ice element particulars

Table 10 shows the particulars for the pack ice sheet elements used in the pack ice numerical model verification tests. A similar table is not provided for the level ice turning circle tests because the only parameter varied was the radius of curvature, which is equal to the vessel element's turning circle radius.

Table 10:   Numerical pack ice elements data sheet.

Test	X1 (m)	X2 (m)	Y1 (m)	Y2 (m)	Floe size (m)	Floe Area (m^2)	Thickness (m)
H25_C5	15	145	-7.5	7.5	2.21	4.8841	0.3783
H25_C6	15	125	-7.5	7.5	2.21	4.8841	0.3783
H25_C7	15	105	-7.5	7.5	2.21	4.8841	0.3783
H50_C6	15	320	-15	15	5.265	27.7202	0.6279
H50_C7	15	275	-15	15	5.265	27.7202	0.6279

Test	Target Conc. (%)	Actual Final Conc. (%)	Conc. Ratio Target (%)	Target Floe Area (m^2)	Final Floe Area (m^2)	Floe Area Ratio Target (%)	Number of Ice Floes
H25_C5	50	50.65	1.013	4.8841	4.889	1.001	202
H25_C6	60	60.4	1.007	4.8841	4.862	0.995	205
H25_C7	70	70.19	1.003	4.8841	4.81	0.985	197
H50_C6	60	59.96	0.999	27.7202	27.848	1.005	197
H50_C7	70	70.15	1.002	27.7202	27.633	0.997	198

5.2   Verification Test Results

Some typical time history plots of the results of the both numerical model verification test results are shown in the following figures.
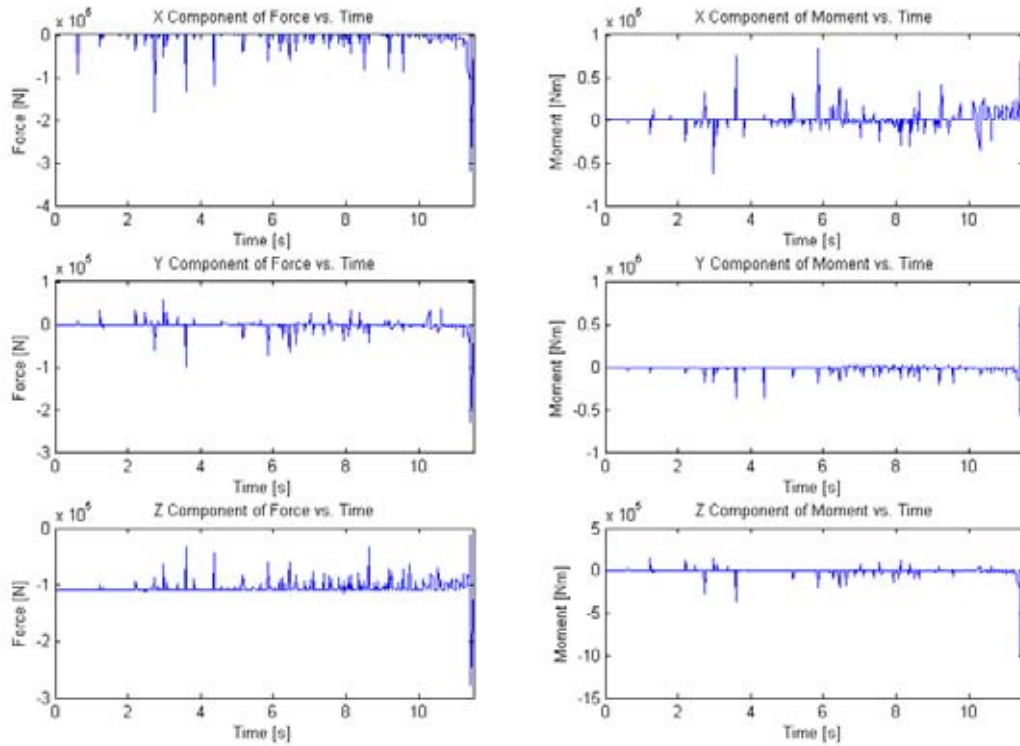
Pack ice resistance tests

Figure 16:   Typical results for pack ice resistance tests with thin ice at 5/10s concentration.
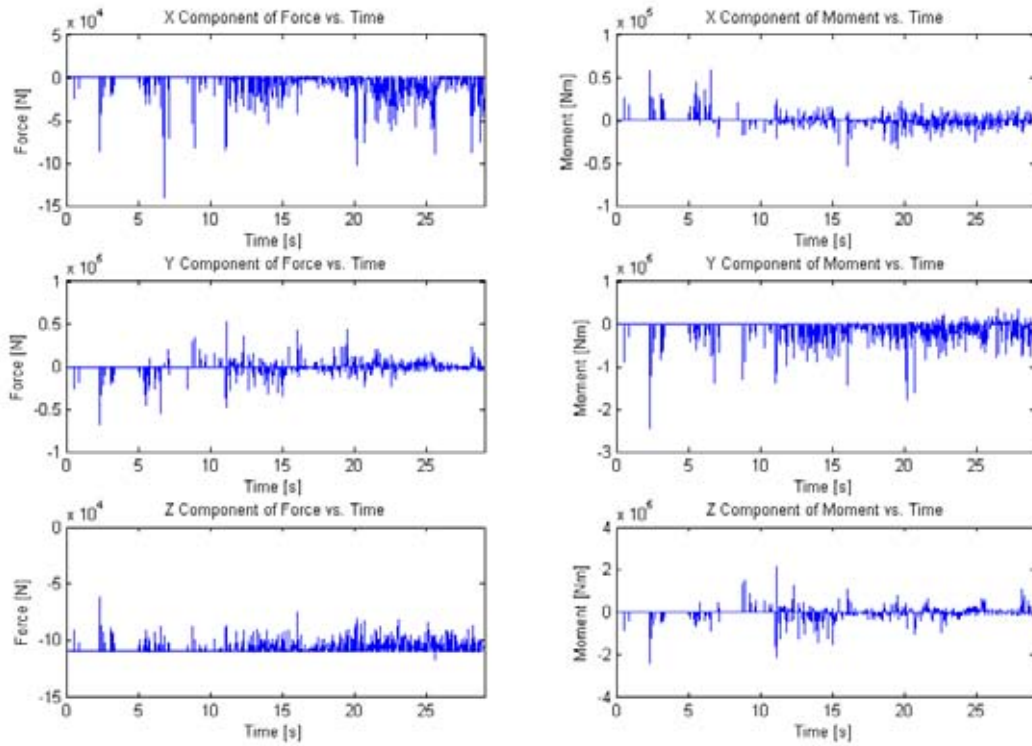
Figure 17: Typical results for pack ice resistance tests with thin ice at 6/10s concentration.

Figure 18: Typical results for pack ice resistance tests with thick ice at 7/10s concentration.
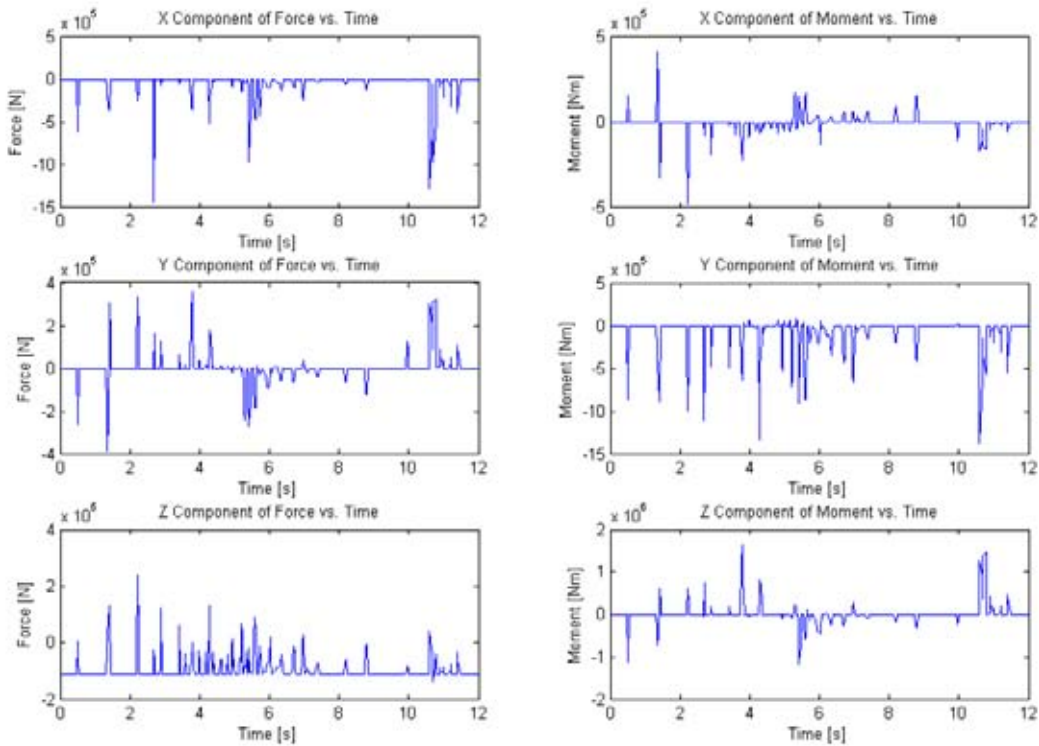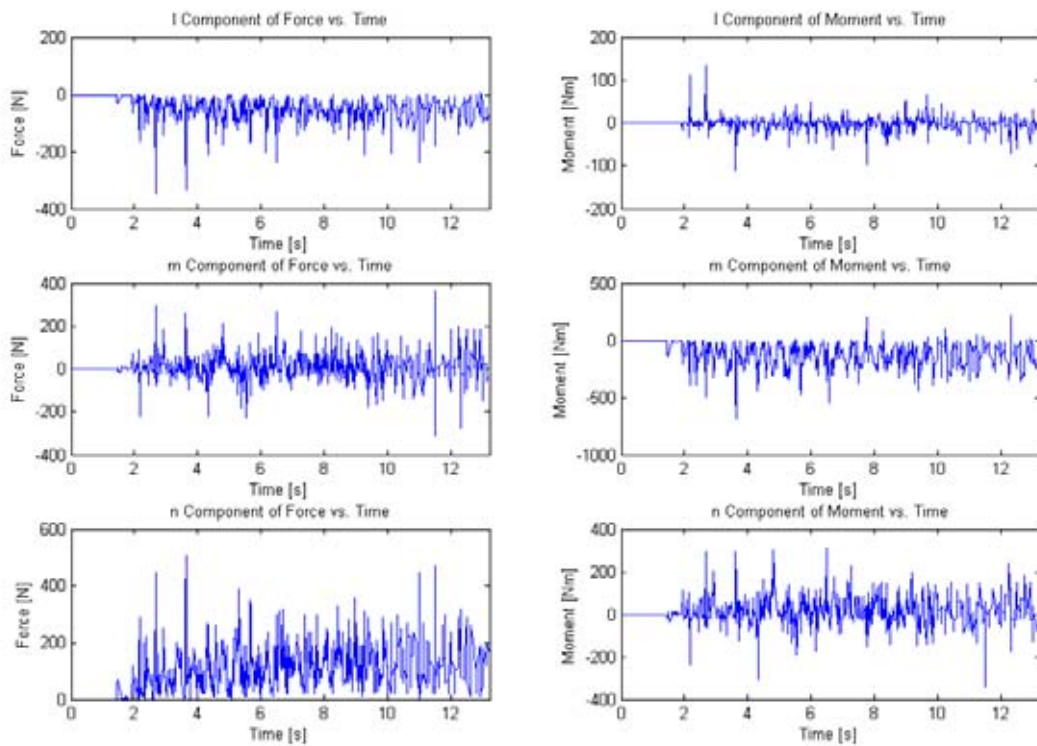
Level ice turning circle tests

Figure 19: Typical results level ice turning circle tests at R = 0 [m] turning circle radius.
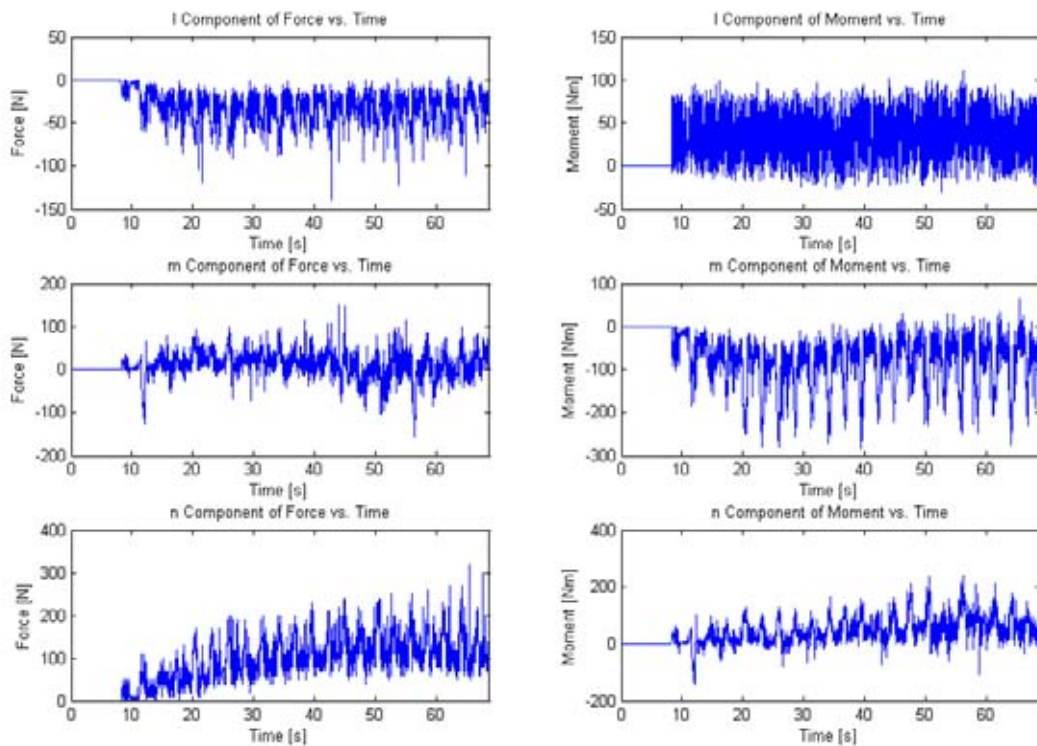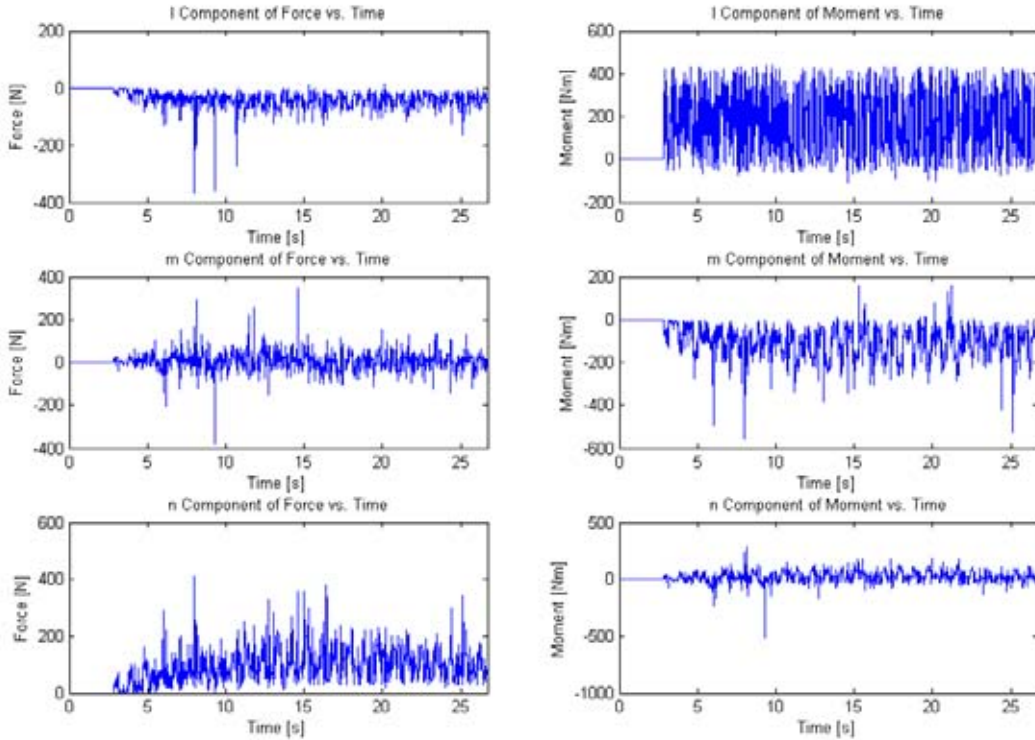

Figure 20: Typical results level ice turning circle tests at R = 10 [m] turning circle radius.

Figure 21:   **Typical results level ice turning circle tests at R = 50 [m] turning circle radius.**

5.3   Numerical and Physical Test Comparison

The simulation results compared very well with their respective measured model test results for both ice performance test types (as can be seen in the following figures).

Figure 22 shows compares the pack ice simulation results with the published model test data (Lau and Simões Ré, 2006). The simulations compared very well for lower ship speeds, and compared favourably for higher ship speeds. Some of the scatter at the higher ship speeds may be due to the random dispersion of the ice floes in both the numerical and physical model tests (i.e. the pack ice may not have been dispersed evenly). This could lead to variation in the results of repeated tests.
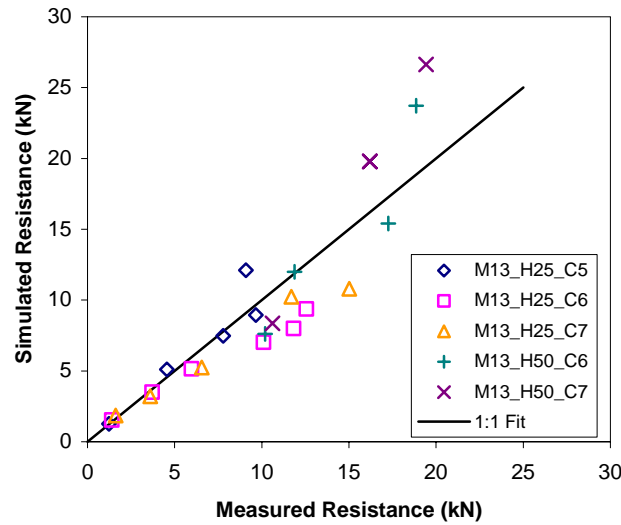
Figure 22: Comparison of pack ice resistance test simulation resistance vs. measured model tests resistance.

With the exception of one point in particular, the results of the level ice turning circle tests compared very well with published data throughout the test matrix (Figure 23). The one outlying point (marked "?" on the figures) is still under investigation. For further comparison, a plot of the yaw moment vs. yaw rate is given in Figure 24 for the DECICE simulations and the published model tests. Again, agreement is very good between the two series' with the exception of the "?" data point.
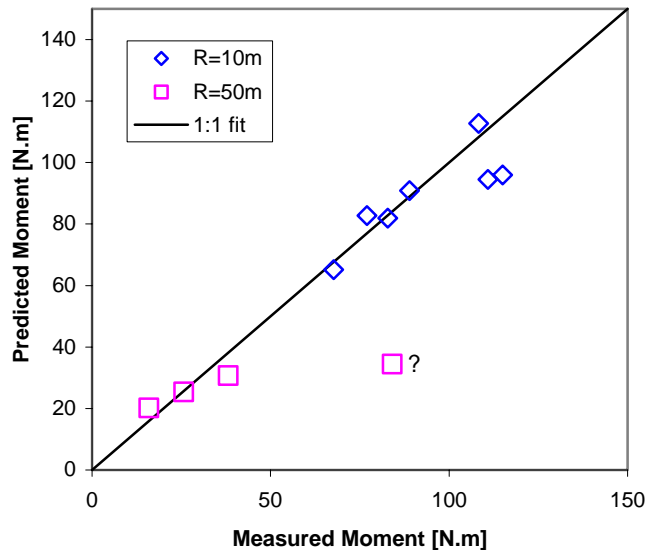
Figure 23: Comparison of level ice turning circle simulation yaw moments vs. measured model test yaw moments.

30
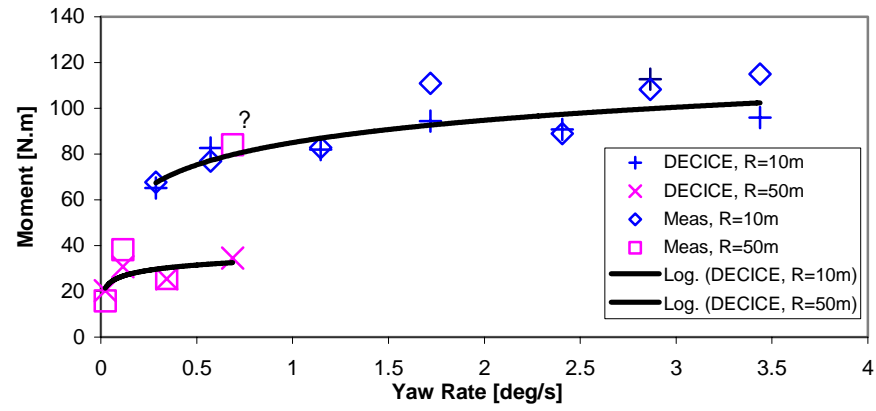
Figure 24: Plot of yaw moment vs. yaw rate for DECICE simulations and measured model test results.

6.0 CONCLUSION

DECICE was used to provide an efficient and feasible means of analyzing vessel performance in ice environments. The underlying logic of DECICE is especially applicable to this type of problem.

Standard methods and techniques for creating numerical models of this type were established, tested, and verified for two well known physical model ice performance tests: Pack ice resistance tests and level ice turning circle tests.

These numerical models provide results that compare very favourably with published model test data; lending confidence to their further development and use as supplementary analysis tools.

7.0 REFERENCES

Babic´, M., Shen, H. T., and H. Bjedov, 1990. "Discrete Element Simulations of River Ice Transport," Proceedings of the IAHR Ice Symposium. Espoo, pp.564-574.

Colbourne, D.B., 2000. "Scaling Pack Ice and Iceberg Loads on Moored Ship Shapes," NRC/IMD Report IR-2000-11, National Research Council of Canada, Institute for Ocean Technology, St. John's, NL, Canada.

Derradji-Aouat, A., and A. van Thiel, 2004. "Terry Fox resistance tests: Phase III, (PMM) Testing ITTC Experimental Uncertainty Analysis Initiative," NRC/IOT Report TR-2004-05, National Research Council of Canada, Institute for Ocean Technology, St. John's, NL, Canada.

Intera Information Technologies: Environmental Division, 1986. "DECICE Theoretical Manual," Intera Information Technologies, Denver, Colorado.

International Towing Tank Conference (ITTC), 1957. Proceedings of the 8th ITTC, Madrid, Spain, published by Canal de Experiencias Hidrodinamicas, El Pardo, Madrid.

Lau, M., 1994a. "A Three Dimensional 'DECICE' Simulation of Ice Sheet Impacting a 60-Degree Conical Structure," NRC/IMD Report CR-1994-16, National Research Council of Canada, Institute for Marine Dynamics, St. John's, NL, Canada.

Lau, M., 1994b. "Pack Ice Jamming Simulation: DECICE2D," National Research Council of Canada, Institute for Marine Dynamics, St. John's, NL, Canada.

Lau, M., McKenna, R.F., Spencer, D., Walker, D. and G.B. Crocker, 1996. "Modelling Pack Ice Forces on Structures from Discrete Floes," Marineering Ltd., St. John's, NL, Canada.

Lau, M., 1999. "Ice Forces on a Faceted Cone due to the Passage of a Level Ice Field," Ph.D. Thesis, Memorial University of Newfoundland, St. John's, NL, Canada.

Lau, M, Phillips, R., McKenna, R.F., and S.J. Jones, 2000. "Discrete Element Simulation of Ridge Keel Resistance during Scouring: A Preliminary Study," Proc. 2nd Ice Scour & Arctic Marine Pipelines Workshop, Mombetsu, Hokkaido, Japan.

Lau, M., and Henley, S., 2004. "DECICE Implementation of Ship Resistance in Ice: Part 1 - Hydrodynamic Modeling," Report LM-2004-16, Institute for Ocean Technology, St. John's, NL, Canada.

Lau, M., 2006. "Discrete Element Modeling of Ship Maneuvering in Ice," 18th International Symposium on Ice, Sapporo, JAPAN (IAHR Ice Symposium 2006), Aug. 28 – Sept. 01, 2006, in preparation.

Lau, M., and A. Derradji-Aouat, 2006. "Phase IV Experimental Uncertainty Analysis for Ice Tank Ship Resistance and Manoeuvring Experiments using PMM," NRC/IOT Report TR-2006-03, National Research Council of Canada, Institute for Ocean Technology, St. John's, NL. Canada.

Lau, M. and A. Simões Ré, 2006. "Performance of Survival Craft in Ice Environments," Performance of Ships and Structures in Ice, ICETECH 2006, July 16-19, Banff, Alberta, Canada.

Løset, S., 1994a. "Discrete Element Modeling of a Broken Ice Field - Part I: Model Development," Cold Regions Science and Technology, Vol. 22, pp.339-347.

Marineering Limited, 1997. "The Development and Commissioning of a Large Amplitude Planar Motion Mechanism for Maneuvering of Ships in Ice and Open Water – Volume 1: Main Report," NRC/IMD Report CR-1997-05 Vol. 1 of 3, Institute for Ocean Technology, National Research Council of Canada, St. John's, NL.

Moaveni, Saeed, 1999. "Finite Element Analysis Theory and Application with ANSYS," Prentice Hall, New Jersey.

Quinton, Bruce, 2004. "Numerical Modeling of a Conventional Lifeboat in Pack Ice," NRC/IOT Report SR-2004-07, Institute for Ocean Technology, National Research Council of Canada, St. John's, NL.

Savage, S. B., 1992. "Marginal Ice Zone Dynamics Modelled by Computer Simulation Involving Floe Collisions," Rep. to the Institute for Mechanical Engineering, National Research Council Canada.

Schachter , M., 1993. "Tess2D – A Tessellation Program", NRC/IMD Report LM-1993-29, National Research Council of Canada, Institute for Ocean Technology, St. John's, NL. Canada.

Simões Ré, A., Veitch, B., Elliott, B., and S. Mulrooney, 2003. "Model Testing of An Evacuation System in Ice Covered Water," NRC/IOT Report TR-2003-03, National Research Council of Canada, Institute for Ocean Technology, St. John's, NL. Canada.

Spencer, D.S. and Timco, G.W., 1993. "CD Model Ice – A Process to Produce Correct Density (CD) Model Ice," Proceedings of the 10th International IAHR Symposium on Ice, Vol. 2, Espoo, Finland, pp. 745-755.

APPENDIX A

PERFORMANCE OF SURVIVAL CRAFT IN ICE ENVIRONMENTS

Michael Lau
Institute for Ocean Technology, National Research Council of Canada
St. John's, NL, Canada
E-mail: Michael.Lau@nrc.gc.ca
Antonio Simões Ré
Institute for Ocean Technology, National Research Council of Canada
St. John's, NL, Canada
E-mail: Antonio.Simoes_re@nrc-cnrc.gc.ca

ABSTRACT

The Institute for Ocean Technology (IOT, formerly the Institute for Marine Dynamics) of the National Research Council of Canada (http://iot-ito.nrc-cnrc.gc.ca/) has conducted physical and numerical simulations of a TEMPSC (Totally Enclosed Motor Propelled Survival Craft) design in ice environments as an integral part of a broader research program that seeks to develop performance standards for Escape, Evacuation, and Rescue (EER) systems in harsh environments. The main objectives of this work are to define practical performance measures for the TEMPSC design in ice covered waters by experimentally investigating the hull's ice transiting resistance and its motions, and to validate a numerical model of lifeboat sail away. This paper reports on the physical model experiments and their comparison with numerical modeling.

KEY WORDS: lifeboat; ice floes; ice load; experiment; numerical.

INTRODUCTION

Oil production and marine transportation off the east coast and in the northern regions of Canada are affected by the presence of ice. Ice is seasonally present at east coast sites and in the event of an emergency it may hamper evacuation. Furthermore, ice is generally present in the north and evacuation systems must be equipped to deal with it. In either case there is very little information related to the performance of survival craft deployed in ice that would allow the development of performance measures or specifications.

The Institute for Ocean Technology (IOT, formerly the Institute for Marine Dynamics) of the National Research Council of Canada (http://iot-ito.nrc-cnrc.gc.ca/) has conducted physical and numerical simulations of a TEMPSC (Totally Enclosed Motor Propelled Survival Craft) design in ice environments as an integral part of a broader research program that seeks to develop performance standards for Escape, Evacuation, and Rescue (EER) systems in harsh environments. The main objectives of this work are to define practical performance measures for the TEMPSC design in ice covered waters by experimentally investigating the hull's ice transiting resistance and its motions, and to validate a numerical model of lifeboat sail away. This paper reports on the physical model experiments and their comparison with numerical modeling.

Three series of model tests were performed in the IOT Ice Tank: launching tests, over-powered sail-away tests, and resistance tests.

These tests were conducted using a 1:13 scale model of the TEMPSC survival craft. The results of the launching and over-powered sail-away tests are published in Simões Ré & Veitch (2003). The present paper documents the results of the resistance tests with the TEMPSC hull design towed at several speeds in open water and in pack ice. The thickness, percentage surface concentration, and floe diameter were varied.

The numerical analysis described in this paper was carried out using DECICE3D, a commercial discrete element code. The discrete element formulation was benchmarked and verified using the experimental data.

This paper presents comparative results showing the effects of various configuration variables on performance, extending from light ice conditions up to extreme ice coverage through numerical simulations and physical model tests. Comparisons between the numerical results and experimental data provide a validation of the numerical model. The work provides a unique, valuable numerical tool to supplement future study of survival craft performance in ice conditions and to provide open water and ice performance profiles of the TEMPSC hull design.

MODEL TESTS

The resistance tests were performed using a specially instrumented lifeboat model (M545) that was attached to the ice tank carriage with a tow post (See Figure 1). The model was constructed of glass-reinforced plastic and was outfitted with a 32mm four-bladed propeller and a steering nozzle. The hydrostatic properties and hull data are summarized in Table 1. The vertical centre of gravity (VCG) and radii of gyration were obtained by swinging the TEMPSC model hull on a frame in air. The free-floating TEMPSC was oscillated in heave, pitch and roll to determine its natural periods and damping coefficients, which are summarized in Table 2.

The tow post was attached at the model's center of gravity and restricted model motion in the yaw and sway directions. These tests were performed such that the lifeboat model was towed at various speeds through enough distance to provide 20 seconds of continuous data. Tests were performed in open water and in ice conditions of varying concentration, floe diameter, and thickness. Determining the resistance versus speed characteristics of open water allowed resistance due solely to ice interactions to be determined. The resistance tests were done following the power tests in the same ice sheets - one at 25 mm nominal ice thickness and one at 50 mm nominal ice thickness. These values correspond to full-scale nominal ice thicknesses of about 0.325 m and 0.650 m, respectively.
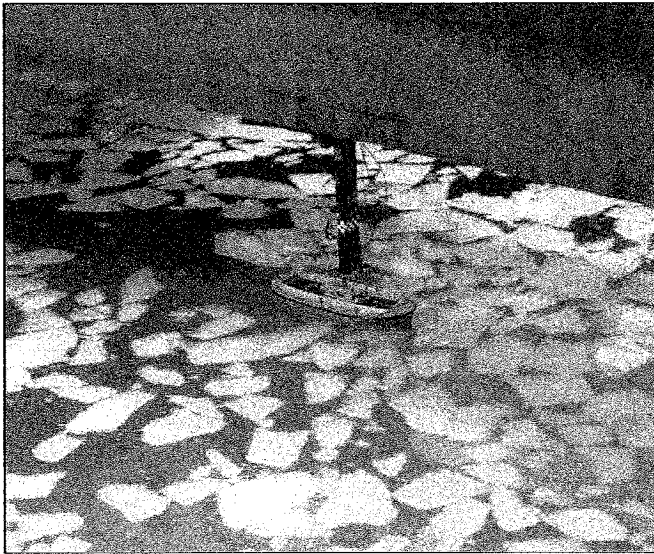
Fig. 1. Resistance test of TEMPSC design in pack ice using PMM

Table 1. Hydrostatic and mass properties of the Totally Enclosed Motor Propelled Survival Craft (TEMPSC) – M545

Property		Full-Scale	1:13 Scale
Length Overall	[m]	10.0	0.769
Beam at Mid-Ship	[m]	3.30	0.259
Displacement	[kg]	11800	5.38
Longitudinal Centre of Gravity	[m]	4.98	0.383
Vertical Centre of Gravity	[m]	1.34	0.103
Draft at Mid-Ship	[m]	0.897	0.069

Table 2. Summary of data obtained for the decay simulations

Test	Experimental Values		Final Values from Simulations	
	ω_n [rad/s]	ζ [kg/s]	ω_n [rad/s]	ζ [kg/s]
Roll	2.15	0.027	2.15	0.027
Pitch	2.43	0.169	2.53	0.162
Heave	3.01	0.167	3.14	0.169

The experiments were carried out using columnar-grained corrected density EG/AD/S ice (Spencer and Timco, 1990). Ice densities were 881 kg/m^3 and 868 kg/m^3 for the 25 mm and 50 mm ice sheets respectively. The pack ice was modeled by initially cutting the level ice in the test area into strips. These strips were then broken apart into ice floes of target size. Removing level ice from the test area border, thereby increasing the water surface area, controlled pack ice concentration. The average flow diameter was computed over selected number of floes assuming circular floe geometry.

Flexural strength of the ice sheet was not a major concern during these experiments as there was no interest in the lifeboat's capability as an icebreaker. However some tempering of the ice was performed to reduce the ice sheet strength to a nominal value of 40 kPa prior to testing.

A total of thirty-two resistance tests were performed: eight open water tests, five in ice at a thickness of 25 mm and 5/10ths concentration, six in ice at a thickness of 25 mm and 6/10ths concentration, five in ice at a thickness of 25 mm and 7/10ths concentration, four in ice at a thickness of 50 mm and 6/10ths concentration, and four in ice at a thickness of 50 mm and 7/10ths concentration.

TEST RESULTS AND DISCUSSIONS

The average resistance for each test run is shown in Figure 2. The total resistance in pack ice is considerably higher than the corresponding resistance in open water. It is clear that the major contributor to the increase in resistance is the ice thickness and floe diameter. Although the ice thickness was confounded with the ice floe diameter, further analysis as shown in this section had suggested large effect of floe diameter on ice resistance. Pack ice concentration appears to be a secondary effect, most noticeable at speeds above 0.5 m/s in the thinner ice. As expected, resistance increased with speed.
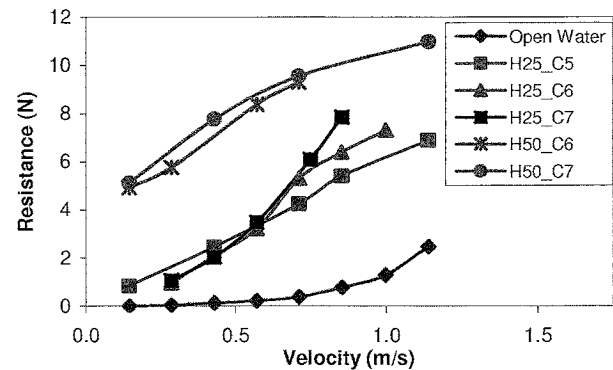

Fig. 2. Model scale total average pack ice resistance vs. velocity (H refers to the thickness, C floe concentration, and B floe diameter)

Results of the resistance tests have been translated to full-scale values for salt water and have been re-analyzed to provide detailed statistical results. In the tests reported here, there was no breaking or significant submergence. Hence, for the calculation of resistance of the TEMPSC through the ice floes, the resistance was divided up into two different components:

$$R_t = R_c + R_{ow} \qquad (1)$$

where: R_c is the resistance due to clearing of ice and R_{ow} is the resistance due to open water.

The clearing component due to pack ice was computed by subtracting the viscous drag on the model (calculating C_f according to the ITTC 1957 Ship Model correlation line). This force component was then non-dimensionalized into an Ice Resistance Coefficient, C_c, and plotted against a non-dimensional speed or Ice Froude Number F_{ni} after Colbourne (2000), who developed a Froude Number based non-dimensional methodology for scaling and analyzing tests of moored

ship shaped vessels subject to ice loads from pack ice or icebergs. His analysis shows that the method provides reasonable data collapse to single curves based on the measured variables. The non-dimensional coefficients are defined as:

$$C_c = \frac{R_c}{\rho_i B h_i V^2 C^3} \quad ^1 \qquad (2)$$

$$F_{n_i} = \frac{V}{\sqrt{ghC}} \qquad (3)$$

where:

ρ_i = density of the ice
B = maximum beam of the model
h = ice thickness (m)
V = TEMPSC velocity (m/s)
g = gravitational acceleration (9.81 m/s^2)
C = pack ice concentration (fraction between 0.5 and 1.0)

Using a viscosity of 1.7866×10^{-6} m^2/s for fresh water at 0°C, and a wetted surface of 190 mm^2 to estimate the viscous drag, the data is plotted as shown in Figure 3 with the following non-dimensional relationship:

$$C_c = 16.1 F_{n_i}^{-1.29} \qquad (4)$$

This mean line derived from a squares fit to the data points can be used to scale the model data to full scale as shown in Figure 4.
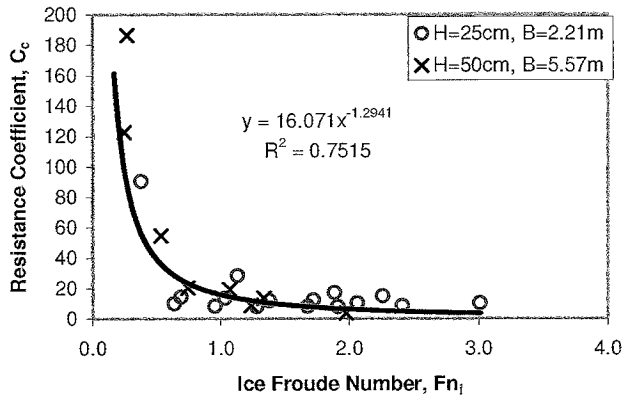

Fig. 3. Data showing pack ice resistance coefficient versus Ice Froude Number (H refers to the thickness and B floe diameter)

Colbourne's formulation does not include effects of floe size. One may expect that clearing of larger floes will be less effective than that of the smaller floes, and hence, it results in a larger clearing force. To examine this hypothesis, the data were grouped into two floe sizes using different symbols in Figure 3.

Within the data scattering the data do not suggest a larger influence of

floe size on the non-dimensional force coefficient (see Figure 3); however, there was not enough floe size variation to allow a firm conclusion.
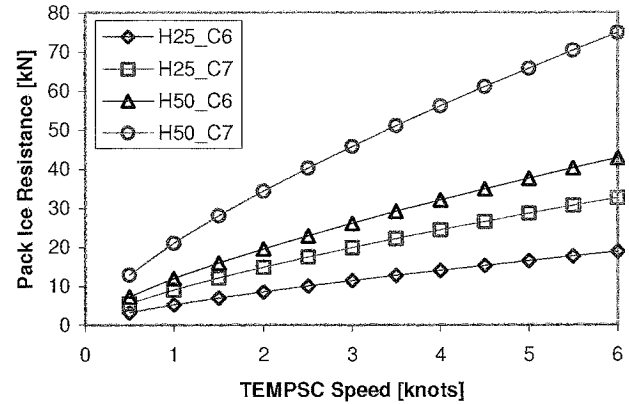

Fig. 4. Full scale pack ice load prediction (H refers to the thickness and C floe concentration)

NUMERICAL MODELING

We are in the process of developing a numerical model using a three-dimensional version of the discrete element code DECICE (Hocking *et al.*, 1987) to investigate the various aspects of the interaction process between a ship and various ice features, including pack ice, level ice, and ice ridges. Various simulation techniques have been developed to closely represent these interactions numerically (Lau and Henley, 2004; Lau and Quinton, 2006). Such analysis is particularly useful to obtain detailed information, i.e. load distribution, energy, and stress states, which cannot be obtained experimentally.

The model presented in this paper was developed for a survival craft transiting in pack ice. The discrete element formulation was first benchmarked and verified using the resistance data of the TEMPSC in open water and in pack ice. We then used the numerical model to study the interaction processes in detail.

The computer program was developed for solving complex solid mechanics problems involving multiple interacting bodies undergoing fracturing. It is presently owned by Oceanic Consulting Corporation and is commercially available. The DECICE computer code is based upon a dynamic equilibrium explicit time stepping formulation and centres around a sophisticated housekeeping logic. The logic is specially designed to track the behaviour and response of a large number of deformable bodies efficiently. The bodies may be in contact with each other while undergoing large non-linear deformation and discrete fracturing. The algorithmic detail of DECICE is described in Hocking *et al.* (1987). The versatility of DECICE in modelling ice-related problems has been demonstrated in a number of recent works by the first author and his colleagues, including ice interactions with a bridge pier (Lau, 1994a), jamming of floes at bridge piers (Lau, 1994b), pack ice forces on structures from discrete floes (Lau *et al.*, 1996), modelling of rubble shear properties and rubble loads exerted on multifaceted cones (Lau, 1999), ridge keel resistance during ice scouring (Lau et al., 2000), and ship manoeuvring in level ice (Lau, 2006).

---

[1] Based on the data for ice transiting vessels, Colbourne's analysis (2000) suggested that a cubic relationship between ice concentration and measured force provides the best data collapse to a mean line.

The Numerical Model

The DECICE simulation was performed at full-scale. The methodology and modeling assumptions used in the interaction model are described with a typical geometrical idealization shown in Figure 5. The discrete element model consists of the following components:

1. A ship model representing the TEMPSC with a prescribed advancing velocity;
2. A mosaic of ice pack with preset concentration modeled with 3-dimensional deformable elements;
3. Boundaries at the rear and sides of the pack ice edge to restrict expansion of the pack ice extent; and
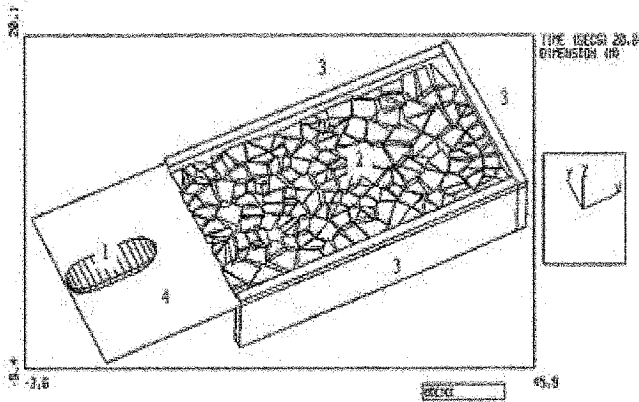4. A water foundation.

Fig. 5. Geometrical idealization of lifeboat in pack ice model used in DECICE simulation: (1-Rigid moving ship; 2-Free-floating pack ice; 3-Rigid Boundary; 4-Water Foundation)

Total run distance for each simulation was set to ten times the ship length to allow sufficient time for the development of a statistically significant ice resistance. The distance was estimated based on experience from previous model tests, and proved to be sufficient.

The TEMPSC Model

The TEMPSC was numerically modeled by a rigid *motion element* (ME) that allows motion in six degrees of freedom. The vessel was modeled without the canopy as only the hull was expected to have contact with the ice/water, and aerodynamic effects were not within the scope of this study. Numerical ballast, trim, decay, and open water resistance tests were performed to ensure that the numerical model results compared favourably with those measured in the model tests.

A series of numerical ballast tests were run in order to verify and fine-tune the draft and trim of the conventional lifeboat numerical model. The mass of the vessel was reduced from 11820 kg to 11220 kg. Additionally, to eliminate the trim of the vessel, the LCG of the vessel was displaced from 4.979 m to 5.157 m.

The second series of hydrostatic tests involved running a number of decay simulations, and attempting to match the simulation results to those obtained in the experimental decay tests. The model's natural frequencies and damping coefficients were re-produced to within 3.5% of the measured values. A detailed procedure for the above hydrostatic matching is given in Lau and Henley (2004).

Pack Ice Model

Pack ice sheets of varying concentration, floe area, and thickness were created using irregular 2D tessellations of 3- and 4-sided convex polygons. For each sheet, the polygons were generated randomly with average polygon (ice floe) area being the controlling parameter. The sum of the areas of these polygons divided by an encompassing rectangular area gives the desired concentration of pack ice. Implementing floe thickness was a simple matter of adding z-direction coordinates to the polygon vertices. Details of the pack ice model are given in Lau and Quinton, 2006.

The pack ice floes were resting on a water foundation. The buoyancy forces and moments acting on each element were calculated by integrating over the wetted surface of each element. The ice floes were modeled using *simply deformable finite elements* (SDFE's) that allow deformation and fracture. In this model, the element is not allowed to fracture. The friction coefficient between ice floes was set to 0.2 as it was the average friction coefficient measured during the physical experiments

Open Water Resistance

To model the open water resistance, a fifth-degree polynomial least squares fit of the resistance vs. speed data collected from the open water resistance tests was performed resulting in the following equation to represent the hydrodynamic resistance of the model:

$$R_{ow} = 21.5V^5 - 154V^4 + 440V^3 - 418V^2 + 217V \qquad (5)$$

The coefficients were entered directly into DECICE to compute open water resistance as a function of velocity. The wave making drag is expected to be proportional to V^4, the smaller constant for V^5 is consistent with this expectation.

Table 3 shows a comparison of the model predictions and the measurements for the open water runs. As shown in the table, the forces measured from the open water tests corresponded rather well to those found in the simulations, especially at higher speeds. The discrepancy found in the run with 0.52 m/s was due to the fact that the trend line used to calculate the values inputted into the numerical model was forced to intercept the origin. Therefore, any small experimental error in the testing would greatly affect the accuracy of values close to origin.

Table 3. Comparison of experimental to simulation tow force in water

Speed [m/s]	Experimental Tow Force [N]	Simulation Tow Force [N]	Error $|(F_s-F_e)/F_e|$ [%]
0.519	32	52	60
1.028	116	112	3
1.543	316	271	14
2.055	496	541	9
2.567	874	955	9
3.079	1724	1658	4
3.595	2858	3008	5
4.010	5446	5577	2

EFFECTS OF DRAG AND SPRING STIFFNESS ON ICE RESISTANCE

When the lifeboat impacts an ice floe, work is done to the ice floe to accelerate it. This work will result in a resistance on the lifeboat of an inertial origin. At the same time, the water drag on the moving ice will impose additional resistance to the lifeboat during the contact. For the inertial component of the ice resistance, the stiffness at the impact interface and the impact velocity are relevant variables, while the ice drag coefficient is important to model the drag force.

The discrete element modeling requires contact springs to transfer loads between elements. The effective normal and tangential spring stiffness of $1x10^7$ N/m^2 was chosen for the present simulation. This value is consistent with those used in Babic′ et al. (1990), Savage (1992), and Løset (1994).

For small ice floes, most of the drag results from unbalanced pressure forces with negligible contribution from fluid friction; hence, only form drag was considered in this simulation with the water drag force and moment being defined, respectively, by:

$$F_D = \frac{C_D V_e^2 \rho_w A_v}{2} \tag{6}$$

$$P_D = \frac{C_D \omega^2 \rho_w A_\omega}{2} \tag{7}$$

where:

C_D = the drag coefficient
V_e = the velocity of the element
ω = the angular velocity of the element
ρ_w = the density of water
A_v and A_ω = element projected "areas" for the vessel element

A value of 1.3 was selected from White (1986) for the drag coefficient. This value is for a rectangular floe with an aspect ratio of 1:10, i.e., for a 0.32 to 0.65 thick floe with a floe size of 2.5 to 5.3 m. To quantify the effect of the drag coefficient and the spring constant on ship resistance, a series of preliminary runs were conducted with these values systematically varied.

Figure 6 shows the effect of drag coefficient on ship resistance for the lifeboat transiting in 50 cm thick pack ice with 6/10ths concentration at various advancing speeds. The numerical predictions correspond to a run distance of 3 lifeboat lengths and a spring constant of $1x10^7$ N/m^2. The computation shows a linear dependency of ice resistance on the drag coefficient and a higher order dependency on ship velocity, consistent with Eqs. 6 and 7. Furthermore, the drag coefficient has negligible influence on lifeboat resistance for these runs. The trend was expected, as the transfer of drag force to the lifeboat would only be possible during initial impact.

Figure 7 shows the effect of spring constant on ship resistance for the lifeboat transiting in 50 cm thick pack ice with 6/10ths concentration at various advancing speed. The numerical predictions correspond to a run distance of 3 lifeboat lengths with a spring stiffness ranging from 1x106 N/m2 to 1x108 N/m2. For these runs, the drag coefficient was set to zero. The result showed a negligible influence of spring stiffness on the resistance within the range of stiffness variation, despite some data scattering. This gives freedom to select a lower spring constant within the examined range of stiffness for computation efficiency.
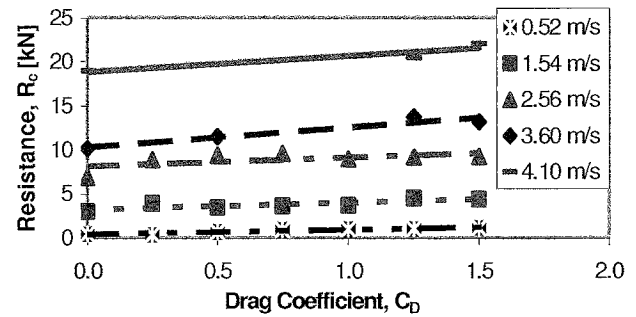

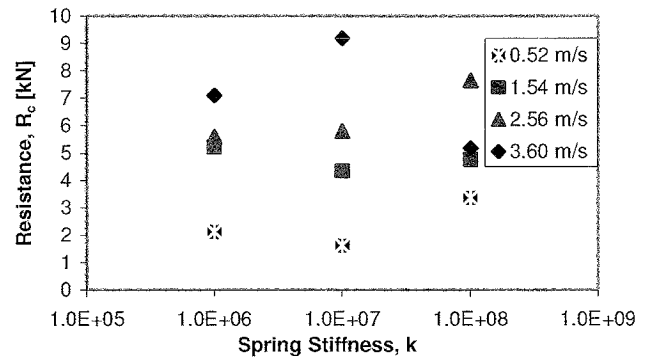Fig. 6. The influence of drag coefficient on pack ice

Fig. 7. The influence of contact spring stiffness on pack ice resistance

EFFECT OF WALL CONSTRAINT ON ICE RESISTANCE

A proper modeling of the boundary condition at the pack ice edge is important for modeling of the pack ice extent. For a practical reason, a finite pack ice extent was modeled. A series of lifeboat transit runs were conducted to assess the effect of wall constraint on lifeboat resistance for the pack ice configuration selected for these simulations. In this series, the sidewalls were progressively relocated away from the pack ice edge to give various degrees of wall constraint. Two 50 cm thick pack ice concentrations of 6/10ths and 7/10ths were used and the lifeboat velocity was 2.56 m/s. Figure 8 shows the effect of the wall constraint on ship resistance. The computation shows a negligible effect of wall constraint on ice resistance for the lower concentration of 6/10ths. It can be shown that this trend is also representative of the thinner ice. This is because the lower concentration allows the lifeboat to push the pack ice around without a significant pack ice build up in front of the lifeboat as shown in Figure 9a. For a higher concentration of 7/10ths, the wall constraint became important as shown by a higher resistance associated with a wall offset of less than 0.25 m. (refer to the first two points in Figure 8.) For these runs, the wall constraint prevented the pack ice to clear from the lifeboat so a large amount of pack ice accumulated in front of and was pushed by the lifeboat as shown in Figure 9b. This accumulation, which was not observed in the model test, was a result of the inaccurate simulation of the pack ice boundary condition. This can be remedied by slightly increasing the wall offset by 50 cm to allow the expansion of the pack ice extent to prevent the ice build up in front of the lifeboat.
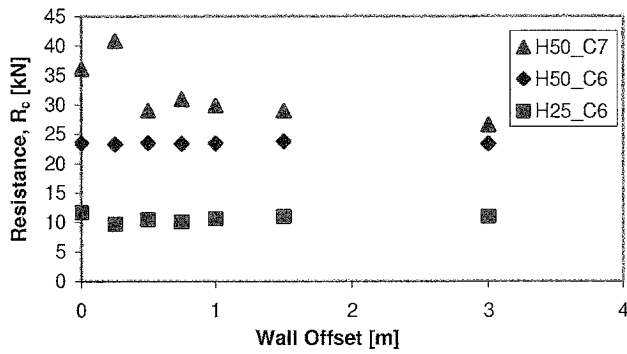
Fig. 8. The influence of ice pack boundary condition on pack ice resistance (V = 2.56 [m/s])
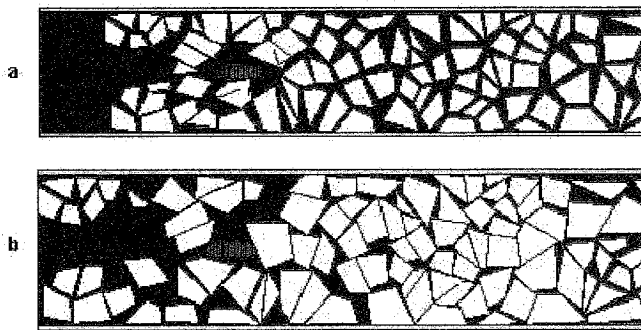

Fig. 9. Small floes with low concentration (a) and large floes with high concentration and accumulation (b)

SIMULATION RESULTS AND DISCUSSIONS

A total of 24 simulations were set up according to the mechanical properties of the ice and the preset TEMPSC velocity for each test run. Details of the simulation are not given here, but some general trends are discussed in the following section.

Figure 10 shows snapshots of a typical simulation for smaller floes with lower ice concentration, and Figure 11 for larger floes with higher ice concentration. Most interaction consisted of a series of discrete ice impact events. During the impact, the pack ice was pushed aside. Some smaller floes may have slid under the hull as shown in Figure 10b. For larger floes, more head-on impact events were observed with a higher chance for the ice to be pushed ahead as shown in Figure 11b. Larger floes and higher concentrations increased the chance for accumulation ahead of the lifeboat with a larger and more intense loading event as shown in Figure 12.
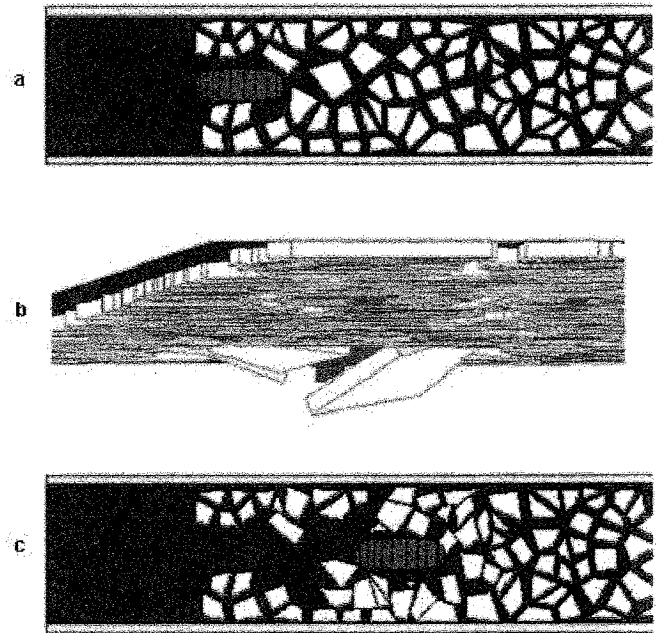

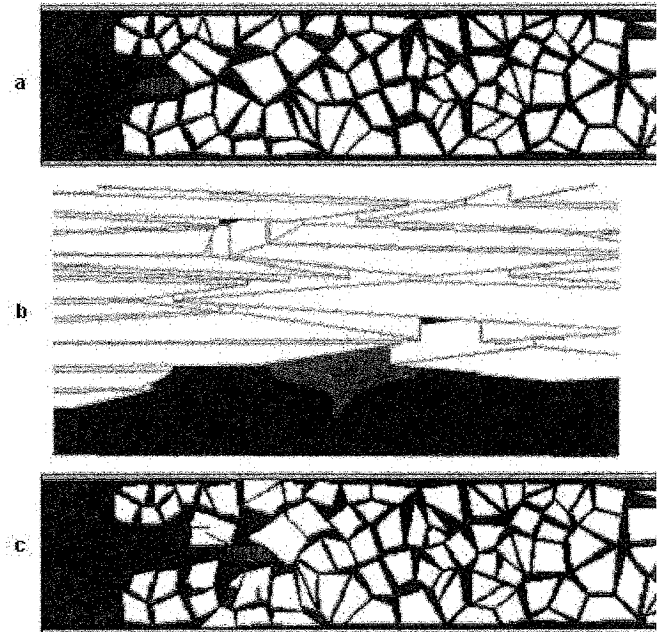Fig. 10. Small floes with low concentration at start time (a), mid run (b), and end time (c)

Fig. 11. Large floes with high concentration at start time (a), mid run (b), and end time (c)
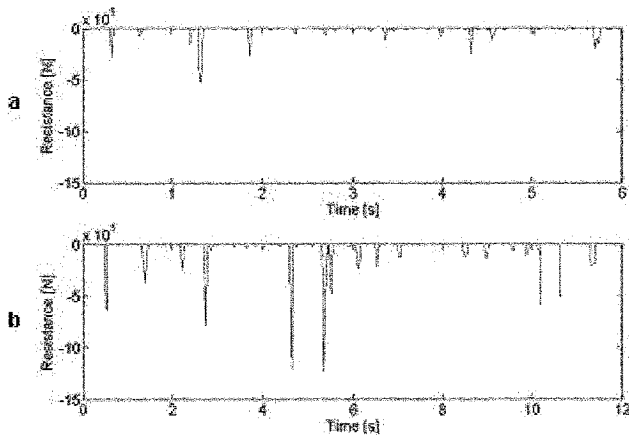
Fig. 12. Time histories of pack ice clearing resistance for small floes of low concentration (a) and for large floes of high concentration (b)

A plot of predicted versus measured resistance is shown in Figure 13. Despite the discrepancy between the simulated ice configuration and that observed in the model test, a good agreement exists between the computed resistance and the experimental measurements. On average, the numerical model slightly underestimates the resistance.
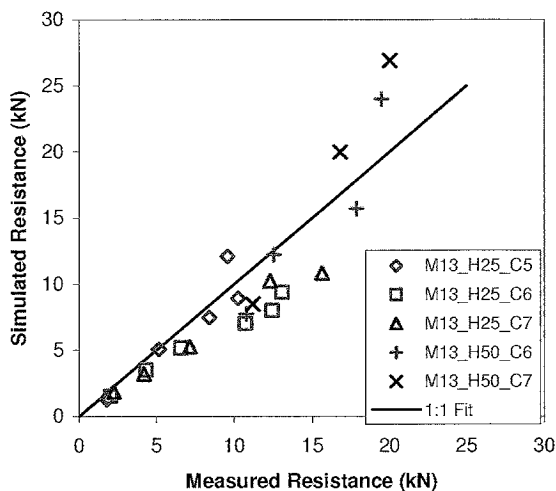

Fig. 13. Comparison of DECICE simulation and model test resistance results

The simulation result for the 4 m/s run with 50 mm ice thickness and 7/10th floe concentration was not included. The numerical prediction for this run was 50kN, while 18 kN was measured from model test. The last discrepancy for this simulation condition may be due to the set-up of the numerical problem, in which the floes were not allowed to fracture. Such condition may not be realistically modelled the test condition, as one would expect ice breaking at this high impacting speed. If the floes were allowed fracturing, the load would be substantially lower.

CONCLUSIONS

This paper reports results of physical model experiments on a conventional TEMPSC model in pack ice and subsequent numerical modeling. The experimental data was non-dimensionalized to provide reasonable data collapse to a single curve. This mean line derived from a squares fit to the data points can be used to scale the model data to full scale. A numerical formulation was developed, benchmarked, and verified using the experimental data. This paper presents comparative results showing the effects of various configuration variables on performance, extending from light ice conditions up to extreme ice coverage through numerical simulations and physical model tests.

Despite a limited amount of experimental data, the numerical analysis gave a favorable prediction. The work has shown that DECICE may be a valuable numerical tool to supplement future study of survival craft performance in pack ice conditions. Future work will include a refinement of the numerical model to include various boat forms, maneuvers, ice features and wave actions, as well as an extensive series of numerical and physical experiments with the aim of defining practical performance measures for the survival craft design in ice covered waters

ACKNOWLEDGMENTS

REFERENCES

Babic', M., Shen, H. T., and H. Bjedov, 1990. "Discrete Element Simulations of River Ice Transport," *Proc. IAHR Ice Sym. Espoo*, pp.564-574.

Colbourne, D. B., 2000. "Scaling Pack Ice and Iceberg Loads on Moored Ship Shapes," *Oceanic Engineering International*, 4 (1): 39-45.

Hocking, G., Mustoe, G.G.W., and J.R. Williams, 1987. "Dynamic Analysis for Generalized Three-Dimensional Contact and Fracturing of Multiple Bodies," *NUMETA*, Balkema Publications, Swansea, UK, 1989.

International Towing Tank Conference (ITTC), 1957. Proceedings of the 8th ITTC, Madrid, Spain, published by Canal de Experiencias Hidrodinamicas, El Pardo, Madrid.

Løset, S., 1994a. "Discrete Element Modeling of a Broken Ice Field - Part I: Model Development," *Cold Regions Science and Technology*, Vol. 22, pp.339-347.

Lau, M., 1994a. " A Three Dimensional 'DECICE' Simulation of Ice Sheet Impacting a 60-Degree Conical Structure," NRC/IMD Report CR-1994-16, National Research Council of Canada, Institute for Marine Dynamics, St. John's, NL, Canada.

Lau, M., 1994b. "Pack Ice Jamming Simulation: DECICE2D," National Research Council of Canada, Institute for Marine Dynamics, St. John's, NL, Canada.

Lau, M., 1999. "Ice Forces on a Faceted Cone due to the Passage of a Level Ice Field," Ph.D. Thesis, Memorial University of Newfoundland, St. John's, NL, Canada.

Lau, M., and Henley, S., 2004. "DECICE Implementation of Ship Resistance in Ice: Part 1 - Hydrodynamic Modeling," Report LM-2004-16, Institute for Ocean Technology, St. John's, NL, Canada.

Lau, M. and Quinton, B., 2006. "DECICE Implementation of Ship Resistance in Ice: Part II – Ship in Pack Ice Modeling," Institute for Ocean Technology, St. John's, NL, Canada.

Lau, M., 2006. "Discrete Element Modeling of Ship Maneuvering in Ice," 18th International Symposium on Ice, Sapporo, JAPAN (IAHR Ice Symposium 2006), Aug. 28 – Sept. 01, 2006, in preparation.

Lau, M., McKenna, R.F., Spencer, D., Walker, D. and G.B. Crocker, 1996. "Modelling Pack Ice Forces on Structures from Discrete Floes," Marineering Ltd., St. John's, NL, Canada.

Lau, M, Phillips, R., McKenna, R.F., and S.J. Jones, 2000. "Discrete Element Simulation of Ridge Keel Resistance during Scouring: A Preliminary Study," *Proc. 2nd Ice Scour & Arctic Marine Pipelines Workshop*, Mombetsu, Hokkaido, Japan.

Simões Ré, A. and Veitch, B., 2003. "Performance Limits for Evacuation Systems in Ice," *Proc. of the 17th international conference on port and ocean engineering under arctic conditions,* POAC '03, Vol. 2, pp. 807-817, Trondheim, Norway.

Savage, S. B., 1992. "Marginal Ice Zone Dynamics Modelled by Computer Simulation Involving Floe Collisions," *Rep. to the Institute for Mechanical Engineering*, National Research Council Canada.

Spencer, D.S., and Harris, C., 1997. "The Development and Commissioning of a Large Amplitude Planar Motion Mechanism for Maneuvering of Ships in Ice and Open Water," Contract Report CR-1997-5, NRC/IOT, St. John's, Nl, Canada.

Spencer, D.S., and Timco, G.W., 1999. "CD Model Ice – a Process to Produce Correct Density (CD) Model Ice," *Proc.10th International IAHR Symp. on Ice*, Vol. 2, Espoo, Finland, pp. 745-755.

White, F. M., 1986. *Fluid Mechanics*, 2nd ed., McGraw-Hill, New York.

APPENDIX B

DISCRETE ELEMENT MODELING OF SHIP MANOEUVRING IN ICE

Michael Lau
Institute for Ocean Technology, National Research Council of Canada,
St. John's, Newfoundland, Canada

ABSTRACT

This paper reports on recent numerical modeling and comparison with physical model experiments conducted in the Institute for Ocean Technology (IOT) of the National Research Council of Canada (http://iot-ito.nrc-cnrc.gc.ca/). The numerical study was carried out using DECICE, a commercial discrete element code. The discrete element formulation has been benchmarked and verified against experimental data from a variety of sources. The numerical simulations conducted in this work include a 1:21 scale model of the Canadian Icebreaker, Terry Fox, advancing and turning in level ice conditions. The physical experiments were carried out in IOT's ice tank using a Planar Motion Mechanism (PMM). Analysis of the numerical results shows the effects of ice conditions and ship motions on the computed forces and moments. Comparisons between the numerical results and experimental data provided a validation of the numerical model.

KEY WORDS: Numerical simulations; Manoeuvring; Sea ice; Model tests; Discrete element method

INTRODUCTION

Recent development of offshore oil and gas reserves in several countries, together with economic studies to increase transportation through the Arctic, has led to a renewed interest in the manoeuvrability of vessels in ice. Despite a sizeable volume of work, there is not yet a universally accepted method of predicting ship performance in ice. The Institute for Ocean Technology (IOT) of the National Research Council of Canada (http://www.iot-ito.nrc-cnrc.gc.ca/) is currently conducting physical, numerical, and mathematical modeling of ship manoeuvring characteristics in ice, as part of a larger effort to develop reliable modeling techniques to assist in the design of new ice-worthy vessels and in the simulation of their navigating characteristics. The objective is to develop a physical representation of the complex interaction processes of a ship manoeuvring in ice and to build mathematical and numerical models to satisfactorily predict its performance. In turn, these models will provide a tool for ship designers to use as part of the assessment of ship navigation in ice infested routes. It can also be incorporated into marine simulators to train mariners, or into automatic ship control systems for better ship manoeuvring.

Lau *et al.* (2006) have presented the numerical modeling of ship navigation performances in pack ice, where ice impact and clearing dominates the interaction. This paper presents results of the numerical analysis on ship manoeuvring in level ice conditions with an added element of complicity - ice failure. Analysis of the numerical results shows the effects of ice conditions and ship motions on the computed forces and moments. Comparisons between the numerical results and experimental data provided a validation of the numerical model. Conclusions are made and recommendations for future works are provided.

NUMERICAL SIMULATIONS

With the advance of computing technology, large simulations are possible even with a small personal computer. Numerical experiments can be useful for understanding complex phenomenon and provide an attractive complementary tool to full-scale measurements and model tests at a fraction of the cost. We are in the process of upgrading a three-dimensional version of the discrete element code DECICE (Hocking *et al.*, 1987) for general ships and structures in ice and wave simulations, including the more complicated tactical operations in ice infested environments, i.e., ships at transit and at berth, iceberg towing, deep sea mooring, seabed scouring, fishing boats and survival craft performance in severe wave and ice environments, etc. Such numerical tool is also useful to obtain detailed information that cannot be obtained experimentally, i.e. load distribution, energy and stress states.
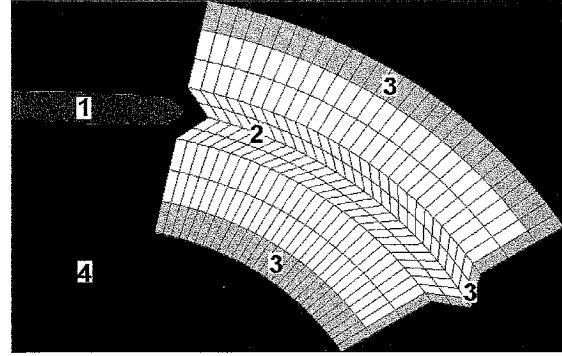
The computer program was developed for solving complex solid mechanics problems involving multiple interacting bodies undergoing fracturing. The versatility of DECICE in modelling ice-related problems has been demonstrated in a number of recent works by the author and his colleagues, including ice interactions with a bridge pier (Lau, 2001), jamming of floes at bridge piers (Lau, 1994), pack ice forces on structures from discrete floes (Lau *et al.*, 1996), modelling of rubble shear properties (Lau, 1999), rubble loads exerted on multifaceted cones (Lau, 1999), ridge keel resistance during ice scouring (Lau *et al.*, 2000), and the performance of survival craft in pack ice (Lau *et al.*, 2006).

The DECICE computer code is based upon a dynamic equilibrium explicit time stepping formulation and centres around a sophisticated housekeeping logic. The logic is specially designed to track the behaviour and response of a large number of deformable bodies efficiently. The bodies may be in contact with each other while undergoing large non-linear deformation and discrete fracturing. The algorithmic details of DECICE are described in Hocking *et al.* (1987).

General Model Description

The methodology and modeling assumptions used in the interaction model are described with a typical geometrical idealization shown in Figure 1. The discrete element model consists of the following components: A ship model representing the Terry Fox with a prescribed turning or advancing motion; a free-floating level ice plate modeled with 3D plate bending elements; fixed blocks at the rear and sides of the ice edge, to model the fixed boundary condition; and a water foundation.

The Terry Fox was numerically modeled by a rigid *motion element* (ME) that allows motion in six degrees of freedom. Numerical ballast, trim, decay, and open water resistance tests were performed to ensure that the numerical model results compared favourably with those measured in the model tests. A standard procedure for the above hydrostatic and hydrodynamic matching is given in Lau *et al.* (2006). For these tests, planar motion of the model was prescribed to simulate that of the model test.

The ice plate consisted of three zones (a central channel and ice area at two sides) with each zone further subdivided into a number of three-dimensional plate bending elements. Elements in the central channel had sides approximately the length of the measured piece size to simulate the observed ice-breaking pattern. This element length to piece size relationship was shown to be satisfactory in simulating the interaction forces in a similar study by Lau (2001).

Figure 1: Geometrical idealization of ship maneuvering model used in DECICE simulation (1 – Rigid moving object; 2 – Free-floating ice plate; 3 – Rigid Boundary; 4 – Water Foundation).

The level ice plate was resting on a water foundation. The buoyancy forces and moments acting on each element were calculated by integrating over the wetted surface of each element. For these simulations, the added masses, moments of inertia, and hydrodynamic damping of the ship were not included. Hence, the computed load represented the ice related components, and the measured open water resistance was subtracted from the total load in ice before comparison with the simulated result.

Total run distance for each simulation was set to double the ship length to allow sufficient time for the development of steady state ice loads. The distance was estimated based on experience from previous model tests, and proved to be sufficient for a preliminary simulation. The open channel width was set according to test measurements. The width of the side ice plate, W, was chosen to be at least three times greater than the characteristic length, l_c, of the ice sheet to properly simulate an ice sheet of infinite extent by a finite boundary. The length L was set to double the ship length plus three times l_c to maintain sufficient distance from the end blocks at the end of the simulation.

For these simulations, a hybrid simple deformable 3-D plate-bending element of the Mindlin type (SDFE) was used. The approach used to derive this type of element is described by Mustoe *et al.* (1987). The ice sheet was modelled as an isotropic elastic brittle material with Mohr-Coulomb failure criteria and tension cut-off. Compressive, shear, tensile, and flexural modes of brittle failure can occur. The elements are fractured along inter-element mesh-lines in the direction given by the fracture criteria and the prevailing stress conditions.

A penalty function approach forms the basis of the contact force generation algorithm implemented in DECICE. A series of stiff contact springs were distributed between the contact interfaces to generate a distribution of contact loading for the two bodies. The spring stiffness was selected to enforce the compatibility condition between elements and give a reasonable time

step length. It was computed from the stiffness of adjacent elements to limit the interface displacement to less than 0.01% of the adjacent element deformations. The normal and tangential inter-element stiffness were chosen equal. The Coulomb friction law limits the magnitude of the shear interaction force between discrete bodies. The external coefficient of ice-ice cohesion was set to zero and the external ice-ice friction coefficient was set to 0.4. The friction between the ice and the model hull was measured and set to 0.01.

Damping was needed to damp the rigid body motions (mass damping) and the internal deformations of SDFE's (internal damping). The fundamental frequencies of rigid body and internal deformation modes of vibration were obtained from a free vibration simulation, in which a vertical impulse was applied on the undamped ice system. The amount of damping in the system was not measured experimentally. Arbitrary values of 5% and 100% critical damping were chosen for the element mass and internal damping, respectively.

The impact of ice on a ship hull involves localized crushing of the ice edge at the immediate contact zone followed by flexural failure. Therefore, a more realistic simulation of the ice failure process would require proper modelling of the localized crushing. This modelling requires a substantial modification of the computer code and is beyond the scope of this study. In the present study, only the existing capabilities of DECICE were employed.

The discrete element modeling requires contact springs to transfer loads between elements. The effective normal and tangential spring stiffness of $3x10^6$ N/m^2 was chosen for the present simulation. A preliminary simulation with an advancing speed of 0.3 m/s and a spring stiffness ranging from $3x10^5$ N/m^2 to $3x10^7$ N/m^2 to assess its effect on yaw moment experienced by the model while performing the 10 m and 50 m turns showed a negligible influence of spring stiffness on the resistance within the range of stiffness variation

MODEL TESTS

The experiments were carried out in CD-EG/AD/S ice with a 1:21.8 scaled model of the Canadian Coast Guard's icebreaker, Terry Fox (IOT Model # 417). The model was mounted to the towing carriage through a PMM (Planar Motion Mechanism) at the model's centre of gravity (see Figure 3), and towed at a controlled planar motion through a level ice sheet. In each experiment tow force, turning moment, and ship motions were measured. The model surface was finished to a friction coefficient of 0.01 with Dupont's Imron paint.

The test matrix for the experimental program is summarized in Table 1. The ice sheets had a target ice thickness of 40 mm and a target flexural strength of 35 kPa. For each ice sheet, flexural, compressive and shear strengths were measured frequently throughout the test period. Turning circle manoeuvring and towed resistance tests were conducted. The constant radius manoeuvre was conducted with two turning radii (50 m and 10 m). All tests were conducted with model velocity ranging from 0.02 m/s to 0.6 m/s. These velocities corresponded with a yaw rate ranging from –0.02 deg/s to –3.4 deg/s. Concurrent to the testing in ice, manoeuvres in open water were also conducted.

Preliminary analysis was performed to understand the observed trend (Lau and Derradji-Aouat; 2004) via mathematical modeling. (See Figure 7.) It is believed that the moment at zero yaw rate were mainly contributed by velocity independent ice breaking and submergence components, and

the slope was determined by velocity dependent ice clearing and the open water components. The readers are referred to Lau and Derradji-Aouat (2004) for details.

Table 1: Matrix of the test program.

Turning Radius, R (m)	∞	50	10
Model Speed, V (m/s)	0.02~0.6		
Yaw Rate, γ (deg/s)	0.02~0.34		
Ice Thickness (mm)	40		
Ice Strength (kPa)	35		
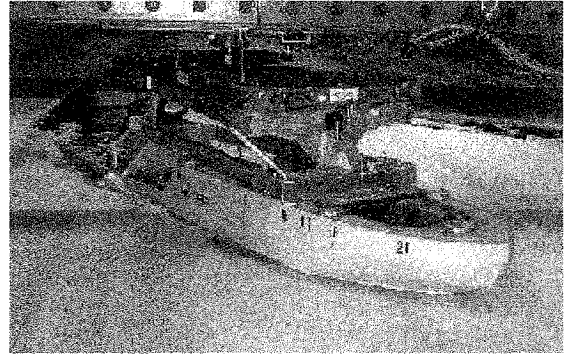
Figure 2: Terry Fox model attached to the PMM.

SIMULATION RESULTS AND DISCUSSIONS

A total of 14 simulations were set up according to the mechanical properties of the ice and the preset ship path for each test run: 11 for ship turning and 3 for ship advancing. An error in the motion controlling software led to a small un-intended drift angle of the model orientation up to 3.8 degrees that increased with yaw rate. The drift angle measured in each test was used in the simulation.

Figure 4 shows snapshots of a typical simulation for ship advancing and for ship turning at the 10 m radius. The interaction consisted of a series of breaking of intact ice and the subsequent submergence and clearing of the broken ice piece typical of those observed in the model tests. The broken ice generated at both sides of the bow clear from the respective side as shown in Figure 5. A typical moment time history of the 50 m and 10 m runs are given in Figures 6a and 6b, respectively.

A plot of predicted versus measured loads is shown in Figures 7a and 7b for the resistance and manoeuvring runs, respectively. Despite the simplicity of the problem treatment, a good agreement exists between the computed loads and the experimental measurements, except one data point corresponding to R = 50 m and V = 0.6 m/s. The computed and measured yaw moments are re-plotted in Figure 8 against yaw rate to further assess the validity of the data point in question. Additional runs were conducted to better define the trends predicted by the numerical model. The computation simulates the trend for R=10 m very well, and in the case of the R=50 m, the first three data points with the lower model speeds give good comparison. The measured value of the data point in question seems not to follow the general trend predicted. It is possible that the measurements for that run were erratic; however, additional data are needed to confirm that.
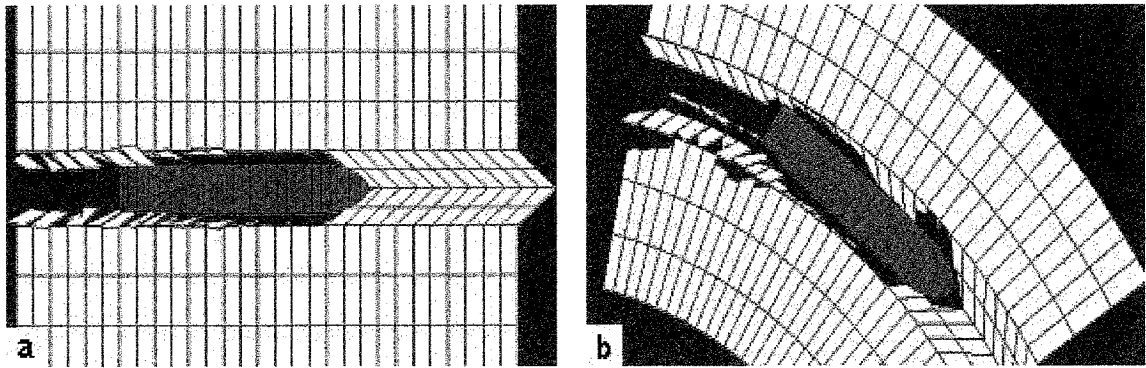
Figure 4: (a) Snapshot of a typical simulation for the ship advancing and (b) for the ship turning at 10 m radius.
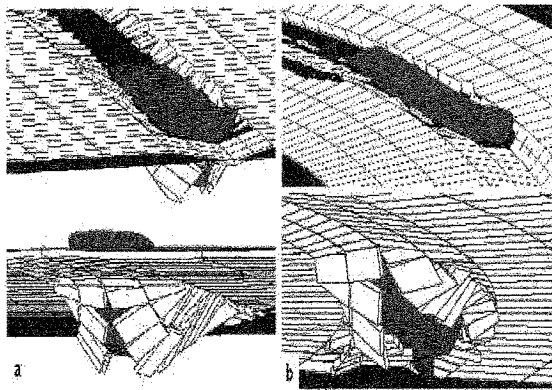

Figure 5: Broken ice clearing for (a) straight advancement and (b) 10 m turning circle radius.
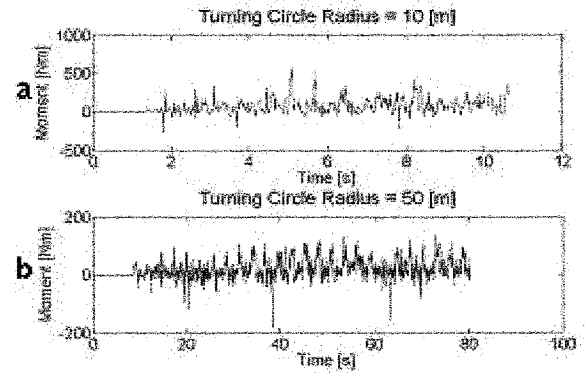

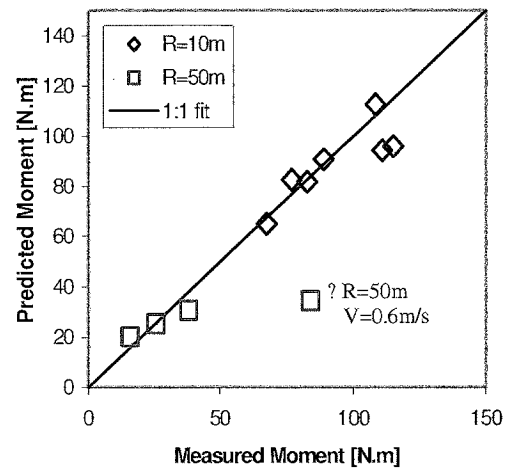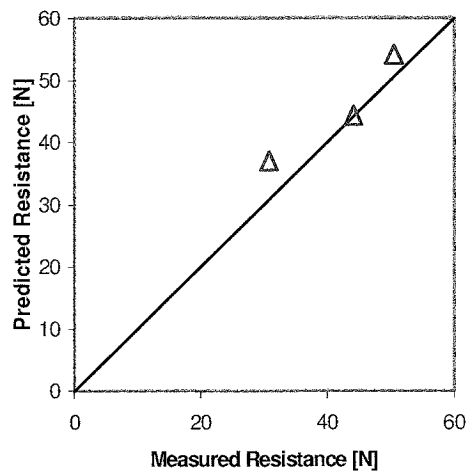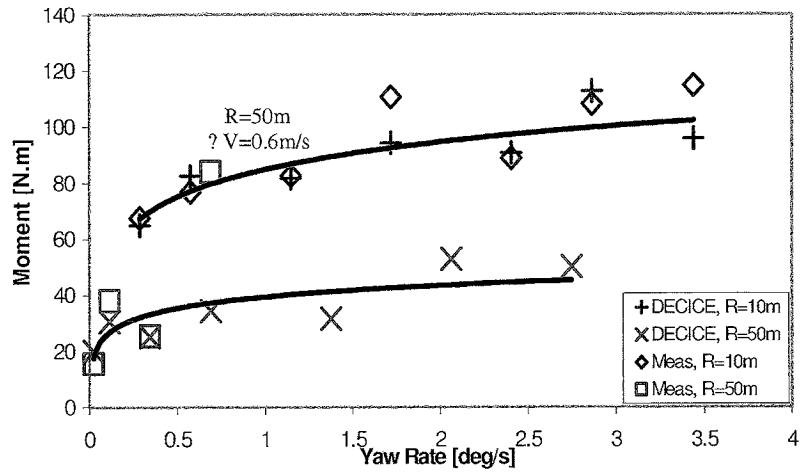**Figure 6:** Typical moment time histories for (a) R=10 m and (b) R=50 m runs.

Figure 7: Predicted versus measured resistance (left) and predicted versus measured moment (right).

Figure 8: Plot of computed and measured yaw moments versus yaw rate.

CONCLUSION AND FURTHER WORK

This paper presents the results of numerical analysis on ship manoeuvring in level ice conditions. The technical approach and methodology employed are briefly described. The validity of the numerical model was assessed by comparing its predictions to measurements from model tests. Analysis of the numerical results shows the effects of ice conditions and ship motions on the computed forces and moments. Comparisons between the numerical results and experimental data provided a validation of the numerical model. Despite the simplicity of the problem treatment, the analysis gave a favourable prediction.

The analysis presented in this paper has been significantly simplified. The elements were not allowed to fail and generate new elements. The crack pattern was imposed according to observation from model tests. This does not allow the ship to create the broken channel according to the prevailing ship motions. Furthermore, a planar motion was also prescribed to the ship in these simulations. Efforts are underway to conduct further simulations to refine the numerical model by: (1) allowing failure of individual ice elements, hence, an arbitrary channel can be created by the ship's prevailing motions, and (2) modeling self propulsion test condition, hence, allowing more realistic ship motions. Details of the ice breaking and clearing processes occurring simultaneously along the hull and the resulting load distributions will also be examined.

ACKNOWLEDGEMENTS

REFERENCES

Hocking, G., Mustoe, G.G.W., and Williams, J.R. (1987), "Dynamic Analysis for Generalized Three-Dimensional Contact and Fracturing of Multiple Bodies", *NUMETA '87*, Balkema Publications, Swansea, UK.

Lau, M. (1999), "Ice Forces on a Faceted Cone due to the Passage of a Level Ice Field," Memorial University of Newfoundland, St. John's, Newfoundland.

Lau, M. (1994), "Pack Ice Jamming Simulation: DECICE2D," National Research Council of Canada, Institute for Marine Dynamics, St. John's, Newfoundland.

Lau, M. and Derradji-Aouat, A. (2004), "Preliminary Modeling of Ship Maneuvering in Ice", 25th Symposium on Naval Hydrodynamics, St. John's, Newfoundland.

Lau, M., McKenna, R.F., Spencer, D., Walker, D. and G. B. Crocker, (1996), "Modelling Pack Ice Forces on Structures from Discrete Floes," Marineering Ltd., St. John's, NF, Canada.

Lau, M., Phillips, R., McKenna, R.F., and Jones, S.J. (2000), "Discrete Element Simulation of Ridge Keel Resistance during Scouring: A Preliminary Study," *Proc. 2nd Ice Scour & Arctic Marine Pipelines Workshop*, Mombetsu, Hokkaido, Japan.

Lau, M., Simões Ré, A., and Veitch, B. (2006), "Performance of Survival Craft in Ice Environments," *International Conference and Exhibition on Performance of Ships and Structures in Ice*, July 16-19, 2006, Banff, Alberta, Canada.

Mustoe, G.G.W., Williams, J.R., Hocking, G., and Worgen, K. (1987), "Penetration and Fracturing of Brittle Plates under Dynamic Impact," *NUMETA '87*, Balkema Publications, July 6-10, Swansea, U.K.